The Misallocation Channel of Climate Change
Evidence from Global Firm-level Microdata

Tianzi Liu* Zebang Xu†

December 23, 2023

Abstract

We document that climate change has a sizable impact on capital misallocation. Using global firm-level microdata from 32 countries, we find causal evidence that temperature-induced capital misallocation is a primary channel through which climate change affects both developed and developing economies. We find that each additional day over 30°C in a year increases the dispersion of marginal products of capital (MRPK), implying a 0.05% decline in annual aggregate TFP under standard elasticities. Moreover, the effect of hot temperature extremes on capital misallocation is worse in more developed countries and hotter regions, suggesting a more significant market cost of climate change with a limited ability to adapt. We develop a firm dynamics model incorporating heterogeneous firm-level climate sensitivity, temperature uncertainty, and damage volatility to explain how an aggregate temperature shock could generate marginal product dispersion. To validate the model's mechanisms, we show that firms' heterogeneous temperature sensitivity, proxied by firm size and adaptability, such as AC installment, creates a differential response of MRPK to temperature shocks. Moreover, we find that temperature affects a firm's TFP volatility non-linearly, and temperature forecast errors in the summer increase capital misallocation. Combining these estimates with the model, we find that the damage volatility channel leads to a TFP loss of 1.27% in our European sample through capital misallocation. Our results suggest an essential role for incorporating firm-level heterogeneity in understanding the aggregate effect of climate change.

*Department of Applied Economics and Management, Cornell University
†Department of Economics, Cornell University

1 Introduction

- Motivation for where our paper stands in literature
- Misallocation has been overlooked in climate-change-economics literature
- In this paper, we decompose the effect into physical productivity and misallocation.
- With orbis, ASI, China firm-level data and ERA5 land weather data. (data introduction, one paragraph)
- We find that temperature is bad for misallocation and misallocation is the major factor.
- We then develop a firm dynamics model to explain the mechanisms and find that two sources of uncertainty brings up firm-level volatility which leads to misallocation.
- Our relation to the literature, 1, 2, 3...
- Structure of the paper.

How does climate change affect the aggregate economy? The existing literature on climate change economics usually treats aggregate productivity losses from temperature variations as worsening technology. At the micro level, empirical work has shown that extreme temperature conditions can affect firm-level productivity, often interpreted as losses of physical productivity (e.g. Zhang et al. 2018; Somanathan et al. 2021). At the macro level, a mix of structural and empirical work prioritizes productivity damage as the primary effect of climate change (e.g. Barrage and Nordhaus 2023; Cruz and Rossi-Hansberg 2023). These works either stay agnostic about the micro origins of the aggregate loss or benchmark their results in efficient economies with little micro-level distortions. However, understanding the sources of the aggregate loss would be essential for the design of adaptation strategies at the micro-level.

Misallocation's role in aggregate productivity has been well-established in the macroeconomic literature since Restuccia and Rogerson (2008) and Hsieh and Klenow (2009), but has been largely overlooked in the context of temperature shocks and climate change. However, the misallocation channel should come as no surprise. While all firms might suffer from climate change, the extent of the damage might vary significantly, with heat-tolerant firms being less affected and more productive than heat-sensitive firms. Therefore, a scenario where more productive and heat-tolerant firms are allocated with less capital than the more heat-damaging firms will feature dispersion in marginal revenue products of capital (MRPK), i.e., misallocation, and results in sub-optimal output levels compared to an efficient economy. As capital is usually considered difficult to adjust in short horizons, many channels, such as a surprise to the temperature that all firms face, would cause such dispersion in capital returns in an economy with heterogeneous temperature sensitivity.

In this paper, we investigate the micro origins of climate-induced aggregate productivity fluctuations. Using global firm-level microdata, we estimate the impact of temperature on technology and capital misallocation. We find that much of the aggregate productivity loss comes from temperature-induced misallocation. Specifically, we show that variations in temperature across short and long horizons increase the dispersion of marginal product of capital among firms, even in a narrowly defined region-sector level. This means that a sizable portion of aggregate climate damage is rooted in the heterogeneity of responses across granular producers in the economy. Moreover, the loss of misallocation is more considerable in hotter regions and more developed economies, suggesting that the market cost of climate change might be higher than previously expected for developed countries.

Our main result can be understood from a climate TFP accounting framework that decomposes aggregate TFP into a set of measurable sufficient statistics, which measures the efficient frontier (i.e., technology) and the dispersion in input and output distortions (i.e., misallocation). These sufficient statistics are assumed to be functions of weather or climate variables. Grounded on the extensive literature on the costs of capital misallocation, we focus on an empirically relevant case where only climate-induced capital distortions are present as a benchmark exercise.

Following our TFP decomposition, the impact of climate conditions on aggregate TFP can be decomposed to the damage of climate conditions on technology and the induced change in capital misallocation. Both channels are easily measurable from firm-level data: technology can be measured as an aggregate of the firm-level Solow residual, while capital misallocation can be measured with the variance of (log) marginal revenue product of capital (MRPK) across firms in a given year.

By compiling comprehensive firm-level micro data covering 32 countries across a wide range of climate conditions across the levels of development, we empirically estimate the causal elasticities of temperature shocks on capital misallocation using computed region-sector level moments ($\mathrm{var}(\log \mathrm{MRPK})$) in a pooled regression. We find significant and robust causal effects of temperature on capital misallocation in both developed and developing economies, indicating that efficiency loss could be the primary driver of aggregate climate damage. Our estimation reveals a U-shape pattern between MRPK dispersion and temperature. Specifically, we find that having an extra day with a temperature above 30°C relative to a day in 5-10°C in a year will increase MRPK dispersion by about 0.4 log points, which translates to 0.05% annual TFP loss from temperature-induced capital misallocation.

A key finding of our empirical estimates is that, when accounting for the heterogeneous effect of temperature-induced misallocation across regional long-run climate and per-capita income levels, the damage of hot temperature extremes on capital misallocation is worse in more developed countries and hotter regions (see in 4a Panel A). The heterogeneous effects of weather on capital misallocation remain strong even if when we restrict our sample to European countries alone, hotter and more advanced economies within the EU see worse impacts of extreme hot events on TFP loss (see in 4b Panel B). This has implications for the estimates of the economic costs of climate damage: richer and hotter countries might suffer more from the misallocation channel, which stands in stark contrast with the other identified channels, suggesting those countries might adapt better.

Our results for the heterogeneous effects across sectors remain consistent with the current estimates in the literature. From the misallocation channel, extreme hot days particularly affect the agriculture and manufacturing sectors. The U-shape pattern also holds for the construction, retail, and services industries, even though it is less statistically significant. Moreover, we also examine the dynamic effect of climate shocks on misallocation via local projection. Relative to the reference category bin of 5-10°C, the effect of a $30°C$ hot day on misallocation is transitory, but the effect of a $< -10°C$ cold day is more persistent. Moreover, we find that the effects are driven by persistence in economic adjustments, not through the persistence in the climate process itself.

To quantitatively understand the importance of the misallocation channel in driving aggregate productivity, we also estimate how temperature shocks affect technology (i.e., Efficient TFP). By comparing the empirical estimates of the technology channel and the misallocation channel, we find that, on average, the misallocation channel contributes more than half to the climate-related decline in region-sector-level aggregate productivity. The misallocation channel is estimated to be one of the leading causes of aggregate TFP loss.

We next develop a firm dynamics model to unpack the drivers behind climate-induced misallocation. In our model, firms are heterogeneous in their average climate sensitivities and face uncertain climate conditions and idiosyncratic climate damages when making dynamic investment decisions. Uncertain climate conditions may increase misallocation because the same unexpected temperature shock may generate differential effects on productivity and MRPK across firms with different levels of adaptation to temperature shocks. Damage uncertainty may increase misallocation because higher-than-optimal temperature increases ex-ante technology volatility, resulting in ex-post input mistakes and generating MRPK dispersion depending on the local realization of damages.

We proceed to examine whether the channels suggested by the model are also grounded in the data. First, we use firm-level panel data to directly examine how identical temperature shocks lead to heterogeneous responses in the MRPK among firms with differing levels of temperature sensitivity. We categorize firms based on their sizes and whether they are equipped with air conditioning (AC) to examine the sources of the heterogeneous temperature sensitivity across firms. Our results indicate that large firms are less damaged than small firms across all temperature ranges. The disparity of log MRPK between small and large firms becomes most economically significant at temperatures exceeding 30°C, which aligns with our empirical evidence that capital misallocation is most affected by extreme heat. This finding also provides insights into our results on heterogeneous effects across varying income levels where richer economies face greater capital misallocation in hot temperatures, as wealthier economies have a higher dispersion in firm sizes as documented by Poschke (2018). Moreover, The India ASI dataset provides a unique opportunity to assess firms' adaptability through survey question that asks whether a firm has installed AC each year. Our results show that firms with AC installations experience insignificant MRPK loss at extreme temperatures, whereas firms lacking AC installations suffer significant MRPK loss under these extreme temperature conditions.

Next, we estimate the quantitative implications of the two channels in the model via model-implied regressions. We first provide direct tests on the relevance of the damage and climate uncertainty channels using region-sector level statistics. By regressing TFP volatility on a polynomial of annual temperatures, we confirm the predictions in our model that temperature acts as a second-moment shock to firm-level TFP. We find that TFP volatility follows a U-shaped pattern with respect to temperature. At an estimated "bliss point" of 13.18°C, TFP volatility reaches the lowest level and posts the lowest burden on allocative efficiency and aggregate TFP. The U-shaped curve also explains why regions with different baseline climates might have heterogeneous misallocation effects from positive temperature shocks, which makes colder regions closer to the "bliss point" while pushing hotter regions further away. Additionally, to test the climate uncertainty channel directly, we employ monthly seasonal temperature forecast data for the EU and test whether aggregated mean squared forecast error affects MRPK dispersion. We find that, conditional on realized temperature, a 1°C temperature forecast error in the warm season (April to September) leads to an increase of 0.97 log points in the variance of MRPK, translating to a 0.13% annual TFP loss.

Lastly, we quantitatively evaluate the effect of the two channels by directly estimating the model-implied expression of MRPK dispersion. We find that, on average, the damage uncertainty channel contributes to 9.5 log points of MRPK dispersion, equivalent to a TFP loss of 1.27%. On the other hand, the climate uncertainty channel's contribution is around 0.0045 and 0.06 log points, implying a TFP loss of 0.06%. The estimates suggest that the level effect of climate change would play a more significant role in raising the productivity costs of misallocation by raising TFP volatility.

Contributions to the Literature. Our study contributes to several strands of literature. Firstly, we contribute to the empirical climate econometrics literature (Dell, Jones, and Olken 2012; Hsiang 2016; Deryugina and Hsiang 2017; Mérel and Gammans 2021; Carleton et al. 2022; Lemoine 2018). These studies have used econometric techniques to estimate the impacts of climate change on various economic outcomes. We extend this literature by proposing a new methodology to derive measurable channel decomposition of climate damage on aggregate TFP. This allows us to isolate the specific channels through which climate change affects the economy. Furthermore, we provide the first causal estimates of temperature on capital misallocation. Our approach provides an empirical framework to link the climate-induced micro-level distortions with the aggregate outcomes.

Secondly, we contribute to the literature on the macroeconomic modeling of climate change (Nath 2023; Nath, Ramey, and Klenow 2023; Cruz and Rossi-Hansberg 2023; Bakkensen and Barrage 2021; Casey, Fried, and Gibson 2022; Rudik et al. 2021). The existing models have incorporated climate change into workhorse macro and trade models of efficient economies. Naturally, these models would be silent on the causes and effects of how climate change would drive distortions and misallocation of productive factors in the economy. This paper provides a static general equilibrium framework to measure the costs of the temperature-induced misallocation channel in general equilibrium via an easy-to-implement sufficient statistics approach. We then develop a heterogeneous firm model to understand the mechanisms behind this effect. In particular, we provide a set-up where the firm-level and cross-sectional TFP volatility depends on the level of temperature, which is a novel micro-foundation of how climate conditions could act as a second-moment shock with strong quantitative implications.

More closely related to our work is the independent and contemporaneous work of Caggese et al. (2023), which studies how temperature shocks affect capital distortions in Italy and uses firm-level estimates to project how aggregate productivity might be affected under different future global warming scenarios. Our work departs from Caggese et al. (2023) along four dimensions. First, rather than making projections, our paper directly identifies the effect of temperature shocks on capital misallocation from historical data across a much more comprehensive range of geographies (EU, China, and India). This, in turn, allows us to accurately estimate the heterogeneous effects of temperature-induced misallocation across countries with different income levels and long-run temperatures. This could be used to accurately project the cost of misallocation channels across regions while accounting for adaptations and future economic development. Secondly, the projection exercise in Caggese et al. (2023) relies on the assumed homogeneous effect of temperature across firms and geographical grids, while our empirical identification requires no such assumptions and allows for explicit heterogeneity to matter. Thirdly, rather than allowing capital to be substitutable and reallocatable across regions and sectors, we identify rising misallocation with temperature extremes within a narrowly defined region-sector pair, which should be interpreted as a lower bound for climate-induced misallocation. Fourthly, by building a firm-dynamics model, our paper explores the endogenous mechanisms through which temperature shocks and long-run climate could drive up capital misallocation and aggregate productivity loss: the nonlinear relationship between TFP volatility and temperature, the heterogeneity of temperature sensitivity across firms, and the role of weather forecast errors. We also identified all these channels directly from the data.

Finally, we contribute to the emerging literature on the causal identification of the drivers of misallocation using (quasi-)natural experiments (Sraer and Thesmar 2023; Bau and Matray 2023). These studies have used exogenous shocks to study the causes and consequences of misallocation. We extend this literature by applying a similar approach to study the effects of climate change. Using large-scale global panel data with highly disaggregated measurements (Province×Sector), we identify the climate drivers of misallocation using a sufficient statistics approach.

Rest of the Paper. The structure of the paper is organized as follows. In Section 2, we develop our climate growth accounting framework. Our data sources and methodology for constructing variables are detailed in Section 3. Section 4 outlines our empirical identification strategy and reduced-form results. Section 5 presents the firm dynamics model to explain the underlying mechanisms. Evidence at the firm level, which tests the proposed channels, is provided in Section 6, and Section 7 offers evidence at the aggregate level. We conclude with Section **??**.

2 A Framework for Climate TFP Accounting

We now develop a framework for TFP accounting in which distortions and productivity endogenously respond to climate conditions. The economic structure here follows the seminal work by Hsieh and Klenow (2009), a closed economy model with heterogeneous firms and input. Our main ? results show how climate conditions affect aggregate productivity in a distorted economy through two distinct channels: micro-level productivity (technology) and the heterogeneity in input/output distortions (misallocation).

2.1 Model Preliminaries

There are N region-sector pairs in an economy. We focus on the aggregation of economic activities within a region-sector pair. Let Y_{nt} denote the aggregate output in a region-sector pair $n = (r, s)$ at year t, where r denotes a region and s denotes a sector.

2.2 Micro effects of Climate Change

We now incorporate climate conditions and temperature variations into our accounting framework. Factor allocations, given a fixed supply of factors within a period, are determined by the fundamentals $(B_{nit}, A_{nit}, \tau^Y_{nit}, \tau^F_{nit})$ for each firm. It is therefore natural to assume these model primitives as endogenous, affected by regional climate and other aggregate[1] or firm-specific economic conditions. These conditions, in turn, determine the equilibrium (mis-)allocation of factors.

Climate Conditions $\mathbf{T}_{rt}$. The climate conditions in region r during year t are represented using a row vector of climate sufficient statistics $\mathbf{T}_{rt}$, with a dimension $1 \times N_T$. This includes data on the realizations of daily temperature, precipitation, and other types of extreme weather events. In our empirical exercise, $\mathbf{T}_{rt}$ will comprise detailed temperature variables and precipitation in year t. The historical record of climate conditions up to year t is denoted as $\tilde{\mathbf{T}}_{rt} = \left(\mathbf{T}_{rt}, \tilde{\mathbf{T}}_{rt-1}\right)$, which combines current year's condition and previous year's history.

Economic Conditions. Similarly, we now characterize the economic states within the economy. We summarize the aggregate state of the region-sector pair as $\mathbf{X}_{nt}$ and the idiosyncratic state of a firm as $\mathbf{Z}_{nit}$, with their history of realization being $\tilde{\mathbf{X}}_{nt} = \left(\mathbf{X}_{nt}, \tilde{\mathbf{X}}_{nt-1}\right)$ and $\tilde{\mathbf{Z}}_{nit} = \left(\mathbf{Z}_{nit}, \tilde{\mathbf{Z}}_{nit-1}\right)$. Both $\tilde{\mathbf{X}}_{nt}$ and $\tilde{\mathbf{Z}}_{nit}$ are assumed to be exogenous to the contemporaneous temperature $\mathbf{T}_{rt}$, yet they may be influenced by the historical climate history $\tilde{\mathbf{T}}_{rt-1}$.

Climate Conditions and Firm-level Fundamentals. We can now establish specific assumptions regarding the impact of climate variables on micro-level elements within the accounting framework. We propose that all firm-level fundamentals are firm-specific and smooth functions based on the realized histories of three key factors: climate conditions ($\tilde{\mathbf{T}}_{rt}$), aggregate economic conditions ($\tilde{\mathbf{X}}_{nt}$), and firm-level state ($\tilde{\mathbf{Z}}_{nit}$). The relationship is represented as follows:

$$A_{nit} = A_{ni}(\tilde{\mathbf{T}}_{rt}, \tilde{\mathbf{X}}_{nt}, \tilde{\mathbf{Z}}_{nit}), \quad B_{nit} = B_{ni}(\tilde{\mathbf{T}}_{rt}, \tilde{\mathbf{X}}_{nt}, \tilde{\mathbf{Z}}_{nit}),$$

$$\tau^Y_{nit} = \tau^Y_{ni}(\tilde{\mathbf{T}}_{rt}, \tilde{\mathbf{X}}_{nt}, \tilde{\mathbf{Z}}_{nit}), \quad \tau^F_{nit} = \tau^F_{ni}(\tilde{\mathbf{T}}_{rt}, \tilde{\mathbf{X}}_{nt}, \tilde{\mathbf{Z}}_{nit}), \quad \forall F \in \{K, L, M\}.$$

It is essential to allow these functions to be firm-specific, allowing the same regional climate conditions $\tilde{\mathbf{T}}_{rt}$ to have varying impacts on elements such as physical productivity, demand, output, and input distortions across different firms within the same region and year. We also allow historical climate conditions, in addition to contemporaneous temperatures, to capture the potentially persistent effect of previous climate conditions and unexpected temperature

1. Here, "aggregate" refers to economic forces that are "common" to all firms in a particular region-sector pair n.

shocks (e.g., $\Delta_{\mathbf{T}_{rt}} = \mathbf{T}_{rt} - \mathbb{E}_{t-1}(\mathbf{T}_{rt}|\tilde{\mathbf{T}}_{rt-1})$ as by Nath, Ramey, and Klenow (2023)).

Industry Production. For each region-sector pair, industrial output Y_{nt} follows a constant elasticity of substitution (CES) production function of J_n differentiated products,

$$Y_{nt} = \left(\sum_{i=1}^{J_n} B_{nit}^{\frac{1}{\sigma_n}} Y_{nit}^{\frac{\sigma_n - 1}{\sigma_n}} \right)^{\frac{\sigma_n}{\sigma_n - 1}}, \tag{1}$$

where $\sigma_n > 1$ is the elasticity of substitution between products within region-sector n, B_{nit} is a good-specific preference shifter, and Y_{nit} denotes the output of firm i. It is assumed that each product is produced by a unique firm. The profit maximization behavior of industrial output producers leads to the inverse demand function for the output of each firm, Y_{nit}:

$$Y_{nit} = B_{nit} Y_{nt} \left[\frac{P_{nit}}{P_{nt}} \right]^{-\sigma_n}, \tag{2}$$

where $P_{nt} = \left(\sum_{i=1}^{J_n} B_{nit} P_{nit}^{1-\sigma_n} \right)^{\frac{1}{1-\sigma_n}}$ is the price index of the region-sector.

Firm-level Production. Firms produce their products with three factors: capital, labor, and materials. They operate with Cobb-Douglas technology,

$$Y_{nit} = A_{nit} K_{nit}^{\alpha_{Kn}} L_{nit}^{\alpha_{Ln}} M_{nit}^{\alpha_{Mn}}, \tag{3}$$

where A_{nit} is physical productivity, K_{nit} is capital stock, L_{nit} is labor input, and M_{nit} is the quantity of materials of the firm. We also assume constant returns to scale in production such that all factor elasticities satisfy $\sum_{F \in \{K,L,M\}} \alpha_{Fn} = 1$. The term A_{nit} can also be interpreted as a measure of quantity-based total factor productivity (TFPQ), reflecting the overall efficiency with which the firm uses its inputs to produce units of physical output[2] (Bils, Klenow, and Ruane 2021).

Subject to the inverse demand, each firm i optimally chooses its quantity of inputs and price to maximize profits:

$$\begin{aligned} \max_{P_{nit}, K_{nit}, L_{nit}, M_{nit}} \; & \left(1 - \tau_{nit}^{Y}\right) P_{nit} \underbrace{A_{nit} K_{nit}^{\alpha_{Ks}} L_{nit}^{\alpha_{Ln}} M_{nit}^{\alpha_{Mn}}}_{Y_{nit}} - \left(1 + \tau_{nit}^{K}\right) R_{nt} K_{nit} \\ & - \left(1 + \tau_{nit}^{L}\right) W_{nt} L_{nit} - \left(1 + \tau_{nit}^{M}\right) P_{nt}^{M} M_{nit} \\ \text{subject to} : \; & Y_{nit} = B_{nit} Y_{nt} \left[\frac{P_{nit}}{P_{nt}} \right]^{-\sigma_n}, \end{aligned} \tag{4}$$

where R_{nt} is the user cost of capital, W_{nt} denotes the wage and P_{nt}^{M} denotes the price for the intermediate input bundles. We consider a general set of firm-specific distortions here. τ_{nit}^{Y} is the price distortion on output faced by firm i, and τ_{nit}^{F} denote the input-specific distortions on factor $F \in \{K, L, M\}$.

2. TFPQ cannot be directly measured in the absence of price or quantity data, barring any additional structural assumptions.

Price distortions τ^Y_{nit} reflect potential heterogeneity in revenue taxes, markups, or prices across firms not captured by the constant Dixit-Stiglitz markup. All input distortions are represented as implicit tax wedges τ^F_{nit} that prevent firms from the ex-post optimal allocation of resources (as if they are paying a higher factor price).[3] In a static framework, τ^F_{nit} represent reduced-form wedges that are endogenous to various mechanisms, including climate change-related ones. We will discuss the endogenous nature of these frictions and their relationship with climate change in Section 5.

Factor Supply. The total productive factors in the region-sector n follows that $K_{nt} = \sum_{i=1}^{J_n} K_{nit}$, $L_{nt} = \sum_{i=1}^{J_n} L_{nit}$ and $M_{nt} = \sum_{i=1}^{J_n} M_{nit}$.

General Equilibrium. The equilibrium allocations in a region-sector depend on the set of fundamentals $(B_{nit}, A_{nit}, \tau^Y_{nit}, \tau^F_{nit})$, $\forall i$ and $\forall F$. Given preference shifter B_{nit}, physical productivity A_{nit}, price distortions $\tau^Y_{nit} < 1$, factor distortions $\tau^F_{nit} > -1$ and total factor supply of K_{nt}, L_{nt}, M_{nt}, a general equilibrium consisting of good prices P_{nit}, factor prices, and equilibrium factor allocation $F_{nit}, F \in \{K, L, M\}$ is defined where all markets clear. We call the equilibrium defined by $(B_{nit}, A_{nit}, \tau^Y_{nit}, \tau^F_{nit})$ the *distorted equilibrium* and the equilibrium defined by $(B_{nit}, A_{nit}, 0, \mathbf{0})$ the *efficient equilibrium*[4] to denote the first best outcome in this economy without distortions.

We now briefly discuss the rationales for our modeling choices.

Physical Productivity, $A_{ni}(\tilde{\mathbf{T}}_{rt}, \tilde{\mathbf{X}}_{nt}, \tilde{\mathbf{Z}}_{nit})$. The impact of temperature on firm-level physical productivity[5] has been established in the literature (Zhang et al. 2018; Nath 2023). The primary findings indicate that extreme heat has a causal effect in reducing physical productivity. We allow A_{ni} to be firm-specific functions of climate conditions, recognizing the highly heterogeneous sensitivity to heat or cold among different types of firms across various sectors and regions. The heterogeneity is potentially attributed to the distinct nature of production processes and varying levels of adaptability to climate conditions as documented in Nath (2023). Therefore, the impact of the same heat shock can vary significantly between firms, with certain types, such as rainfed farms, potentially suffering more than others, like irrigated farms. To be consistent with established models of firm dynamics and misallocation, e.g., Hopenhayn (1992), Asker, Collard-Wexler, and Loecker (2014), and Moll (2014), we also allow aggregate and firm-specific economic states to affect A_{nit}.

Demand Shifter, $B_{ni}(\tilde{\mathbf{T}}_{rt}, \tilde{\mathbf{X}}_{nt}, \tilde{\mathbf{Z}}_{nit})$. Firms' exposure to climate conditions also stems from demand-side effects, especially in developed economies in which leisure and recreational activities are important in the consumption basket. This is evident in industries where climate variations directly affect consumer behavior. For instance, in the service industry, Zivin and Neidell (2014) found that Americans are more likely to shift to indoor recreational activities

3. For a firm to be productive, it is necessary that all prices are positive, which requires $1 - \tau^Y_{nit} > 0$ and $1 + \tau^F_{nit} > 0$.
4. Efficient in an unconstrained sense (as defined by Carrillo et al. 2023).
5. In a Cobb-Douglas framework, this also includes labor productivity.

from outdoor ones (such as recreational fishing (Dundas and Haefen 2020)) when exposed to heat shocks. The revenue productivity change of the related firms is not due to changes in the firms' physical productivity but rather to a shift in market demand influenced by climatic conditions.

Output Distortion, $\tau^Y_{ni}(\tilde{\mathbf{T}}_{rt}, \tilde{\mathbf{X}}_{nt}, \tilde{\mathbf{Z}}_{nit})$. Output distortion, represented by τ^Y_{nit}, captures the distortions the firm faces on prices/quantities relative to the CES benchmark. These distortions can arise from policy interventions, market imperfections, or other externalities. For example, regulations and subsidies designed to aid an economy damaged by climate conditions might impose additional costs or benefits on production. Moreover, market structure, including firm-specific market power and profitability, might also be influenced by climate conditions (Cascarano, Natoli, and Petrella 2022).

Input Distortions, $\tau^F_{ni}(\tilde{\mathbf{T}}_{rt}, \tilde{\mathbf{X}}_{nt}, \tilde{\mathbf{Z}}_{nit})$. This paper mainly focuses on how climate conditions affect input distortions. For any input $F \in \{K, L, M\}$, the firm's optimality condition with respect to F_{it} will yield that the marginal revenue product of factor F (MRPF) equals to:

$$MRPF_{nit} = \alpha_{F_n} \frac{\sigma_n}{\sigma_n - 1} \frac{P_{nit} Y_{nit}}{F_{nit}} = \frac{1 + \tau^F_{ni}(\tilde{\mathbf{T}}_{rt}, \cdot)}{1 - \tau^Y_{ni}(\tilde{\mathbf{T}}_{rt}, \cdot)} P^F_{nt}, \tag{5}$$

which states that any shift in climate conditions would affect the input (and output) wedges and distort the firm input choices F_{nit} as well as MRPF. Moreover, any heterogeneity in the input or output distortions response to temperature would result in unequal marginal revenue return to factors among firms, i.e., "misallocation." We can explicitly link these distortions to equilibrium (mis-)allocation of resources as follows.

Proposition 1 ***Equilibrium (Mis-)allocation.*** *The distorted equilibrium allocation of capital, labor, and material inputs must satisfy that for any $F \in \{K, L, M\}$,*

$$\begin{aligned}\log\left(\frac{F_{nit}}{F^*_{nit}}\right) = &-\log(1 + \tau^F_{ni}(\tilde{\boldsymbol{T}}_{rt}, \cdot)) + \sigma_n \log(1 - \tau^Y_{ni}(\tilde{\boldsymbol{T}}_{rt}, \cdot)) \\ &- (\sigma_n - 1) \sum_{F'=\{K,L,M\}} \alpha_{F'_n} \log(1 + \tau^{F'}_{ni}(\tilde{\boldsymbol{T}}_{rt}, \cdot)),\end{aligned} \tag{6}$$

where F^*_{nit} is the efficient equilibrium allocation of factors that are entirely determined by preference shifter and physical productivity within the region-sector:

$$F^*_{nit} = \frac{B_{ni}(\tilde{\boldsymbol{T}}_{rt}, \cdot) A_{ni}(\tilde{\boldsymbol{T}}_{rt}, \cdot)^{\sigma_n - 1}}{\sum_j B_{nj}(\tilde{\boldsymbol{T}}_{rt}, \cdot) A_{sj}(\tilde{\boldsymbol{T}}_{rt}, \cdot)^{\sigma_n - 1}} F_{nt}$$

Proof. See Appendix. ■

In an efficient economy free of distortions, climate only affects preferences and physical productivity, leading to a resource allocation favoring firms whose products are preferred by customers and those with higher physical productivity. However, in a distorted equilibrium with temperature-sensitive wedges, temperature shocks (the change in $\mathbf{T}_{rt}$) can affect input and output wedges, resulting in a state of misallocation of F_{nit} compared to the efficient counterpart F^*_{nit}. $\log(\frac{F_{nit}}{F^*_{nit}})$ decreases with factor-specific wedges $\log(1+\tau^F_{ni}(\tilde{\mathbf{T}}_{rt},\cdot))$ due to increased effective cost of the factor, increases with output wedge from greater price incentives, and decreases with the distortions of all other factors (i.e., "mixed" distortions), $\sum_{F'=\{K,L,M\}} \alpha_{F'_n} \log(1+\tau^{F'}_{ni}(\tilde{\mathbf{T}}_{rt},\cdot))$[6], as higher costs of one factor would lead to reduced usage of other factors.

In the context of temperature effects, consider this example: if firm A's capital wedge increases with the current temperature (a variable in $\tilde{\mathbf{T}}_{rt}$), while firm B's decreases, a temperature shock would raise the effective price of capital for firm A. As a result, firm A would allocate less capital than is efficient for its production compared to firm B.

Input wedges could be endogenous of temperature due to its interactions with a variety of well-established mechanisms, including adjustment costs (Asker, Collard-Wexler, and Loecker 2014), financial frictions (Moll 2014; Gopinath et al. 2017; Bigio and La'O 2020), information frictions (David, Hopenhayn, and Venkateswaran 2016; Chahrour, Nimark, and Pitschner 2021). In more realistic investment decision settings, capital appears as a dynamic input that must be invested before the actual climate conditions are known. Therefore, any unexpected changes in climate conditions would unambiguously shift the actual return away from the expected return, which appears as input distortions in the ex-post measurement, as conducted in our analysis.

We will remain agnostic on the endogenous mechanism for now and leave the detailed discussion and identification of mechanisms driving the climate-induced distortions in Section 5, 6, and 7.

2.3 Aggregation, TFP Decomposition and Misallocation

We proceed to perform aggregation in this accounting framework. We adopt a widely-used assumption in the misallocation literature (see Hsieh and Klenow 2009 and Sraer and Thesmar 2023). This assumption suggests that productivity and all associated wedges follow a joint log-normal distribution (Shapiro-Wilk test to be added) across firms in any region-sector-year, which holds very well in the data. More formally, we consider a set of functions $\{B_{ni}, A_{ni}, \tau^Y_{ni}, \tau^F_{ni}\}$ for all i and F. We assume that for any given set of arguments $\left(\tilde{\mathbf{T}}_{rt}, \tilde{\mathbf{X}}_{nt}, \left\{\tilde{\mathbf{Z}}_{nit}\right\}_i\right)$, the joint distribution of the realized values of these functions, denoted as $\mathbf{S}_{nit} = \left(B_{nit}, A_{nit}, 1+\tau^Y_{nit}, 1+\tau^K_{nit}, 1+\tau^L_{nit}, 1+\tau_{i}\right.$ can be characterized as follows:

$$\log(\mathbf{S}_{nit}(\tilde{\mathbf{T}}_{rt}, \tilde{\mathbf{X}}_{nt}, \tilde{\mathbf{Z}}_{nit})) \sim \mathcal{N}\left(\mu^{(n)}_s(\tilde{\mathbf{T}}_{rt}, \tilde{\mathbf{X}}_{nt}), \Sigma^{(n)}_{ss}(\tilde{\mathbf{T}}_{rt}, \tilde{\mathbf{X}}_{nt})\right) \tag{7}$$

Here, $\mu^{(n)}_s$ represents the mean vector of firm-level fundamentals, while $\Sigma^{(n)}_{ss}$ is the covariance matrix of these fundamentals across firms. Both of these parameters are smooth functions of their respective arguments. This smoothness follows the principle that population moments are smooth functions of the variables $\mathbf{S}_{nit}$. For tractability, we adopt the aggregation notation of Krusell and Smith (1998) that the distribution of $\tilde{\mathbf{Z}}_{nit}$ (over i) can be summarized by a finite set of moments and stacked into the aggregate states of the economy $\tilde{\mathbf{X}}_{nt}$. The log-normality as-

6. This holds as long as goods are substitutable, i.e. $\sigma_n > 1$

sumption is particularly desirable to study the aggregate properties of the micro-level wedges and productivity:

Proposition 2 ***Aggregation and TFP Decomposition.*** *Under the log-normality assumption, each region-sector n admits an aggregate production function of the form*

$$Y_{nt} = TFP_{nt} K_{nt}^{\alpha_{Kn}} L_{nt}^{\alpha_{Ln}} M_{nt}^{\alpha_{Mn}}, \tag{8}$$

where the region-sectoral aggregate Total Factor Productivity function $TFP_{nt} := TFP_n\left(\tilde{\mathbf{T}}_{rt}, \tilde{\mathbf{X}}_{nt}\right)$ can decomposed as following:

$$\begin{aligned}
\log TFP_n(\tilde{\mathbf{T}}_{rt}, \cdot) = &\underbrace{\frac{1}{\sigma_n - 1} \log \mathbb{E}_i \left[B_{ni}(\tilde{\mathbf{T}}_{rt}, \cdot) \left(A_{ni}(\tilde{\mathbf{T}}_{rt}, \cdot) \right)^{\sigma_n - 1} \right]}_{Technology (\log TFP_n^E)} - \underbrace{\frac{\sigma_n}{2} \operatorname{var}_{\log\left(1-\tau_{ni}^Y\right)}(\tilde{\mathbf{T}}_{rt}, \cdot)}_{Output\ Wedge\ Dispersion} \\
&- \underbrace{\sum_{F \in \{K,L,M\}} \frac{\alpha_{Fn} + \alpha_{Fn}^2(\sigma_n - 1)}{2} \operatorname{var}_{\log\left(1+\tau_{ni}^F\right)}(\tilde{\mathbf{T}}_{rt}, \cdot)}_{Factor\ Wedge\ Dispersion} \\
&+ \underbrace{\sigma_n \sum_{F \in \{K,L,M\}} \alpha_{Fn} \operatorname{cov}_{\log\left(1-\tau_{ni}^Y\right), \log\left(1+\tau_{ni}^F\right)} \left(\tilde{\mathbf{T}}_{rt}, \cdot \right)}_{Output\text{-}Factor\ Mixed\ Distortion} \\
&- \underbrace{(\sigma_n - 1) \sum_{F \in \{K,L,M\}} \sum_{F' \neq F} \alpha_{Fn} \alpha_{F'n} \operatorname{cov}_{\log\left(1+\tau_{ni}^F\right), \log\left(1+\tau_{ni}^{F'}\right)} \left(\tilde{\mathbf{T}}_{rt}, \cdot \right)}_{Factor\ Mixed\ Distortion}
\end{aligned} \tag{9}$$

Proof. See Appendix. ■

All the variance and covariance terms are elements in the variance matrix $\Sigma_{ss}^{(n)}(\tilde{\mathbf{T}}_{rt}, \tilde{\mathbf{X}}_{nt})$ in Equation 7. Each is a region-sector-specific function of weather conditions and other economic fundamentals.

Notice that in the absence of distortions, we will have the efficient level of TFP, $\log \text{TFP}_n^E = \frac{1}{\sigma_n - 1} \log \mathbb{E} \left[B_{ni}(\tilde{\mathbf{T}}_{rt}, \cdot) \left(A_{ni}(\tilde{\mathbf{T}}_{rt}, \cdot) \right)^{\sigma_n - 1} \right]$, determined by the preference shifter and love-for-variety-adjusted physical productivity of the firm. This represents the production possibility frontier of the economy. We call this **technology** in the spirit of Basu and Fernald (2002) and Baqaee and Farhi (2019).

The rest of the terms represent the costs of distortions in the economy, referred to as **misallocation loss**. Dispersion in output wedges $\operatorname{var}_{\log\left(1-\tau_{ni}^Y\right)}$ and factor input wedges $\operatorname{var}_{\log\left(1+\tau_{ni}^F\right)}$ will both lead to dispersion in the marginal revenue product of factors, creating more misallocation of factors, which lowers the level of TFP. Moreover, wedge dispersion will be more costly if the products are more substitutable (i.e., higher σ_n) as gains from reallocation would be larger. Also, factor wedge dispersion on factors of greater importance in production (higher α_{F_n}) will be more costly.

Furthermore, the interactions of the wedges matter as well. All else equal, productivity loss from wedges will be larger if lower markups firms also face larger input distortions ($\text{cov}_{\log(1-\tau^Y_{ni}),\log(1+\tau^F_{ni})} < 0$). Similarly, the cost of misallocation will be higher if capital-distorted firms are also likely to be those facing higher labor distortions ($\text{cov}_{\log(1+\tau^F_{ni}),\log(1+\tau^{F'}_{ni})} > 0$). These interactions are often referred to as "mixed" distortions.

2.4 Decomposing the Impact of Climate Change on TFP

Our decomposition framework shows that aggregate TFP depends on moments concerning technology and misallocation, which are endogenous to climate conditions. Since we have assumed that all moments are smooth functions of climate conditions $\tilde{\mathbf{T}}_{rt}$, we can decompose the first-order impact of climate change on TFP via a set of causal elasticities for each relevant moment. We formalize this via the following proposition:

Proposition 3 ***Climate conditions and TFP.*** *Under the log-normality assumption, the first-order impact of climate conditions $\tilde{\mathbf{T}}_{rt}$ on region-sectoral aggregate TFP can be decomposed as:*

$$
\begin{aligned}
\frac{\partial \log TFP_n(\tilde{\mathbf{T}}_{rt},\cdot)}{\partial \tilde{\mathbf{T}}_{rt}} &= \frac{\partial\, \textit{Technology}_{nt}}{\partial \tilde{\mathbf{T}}_{rt}} - \frac{\partial\, \textit{Misallocation Loss}_{nt}}{\partial \tilde{\mathbf{T}}_{rt}} \\
&= \frac{1}{\sigma_n - 1} \frac{\partial \log\left(\int B_{ni}(\tilde{\mathbf{T}}_{rt},\cdot)\left(A_{ni}(\tilde{\mathbf{T}}_{rt},\cdot)\right)^{\sigma_n-1} di\right)}{\partial \tilde{\mathbf{T}}_{rt}} - \frac{\sigma_n}{2}\frac{\partial\, \text{var}_{\log(1-\tau^Y_{ni})}(\tilde{\mathbf{T}}_{rt},\cdot)}{\partial \tilde{\mathbf{T}}_{rt}} \\
&\quad - \sum_{F\in\{K,L,M\}} \frac{\alpha_{Fn} + \alpha^2_{Fn}(\sigma_n - 1)}{2} \frac{\partial\, \text{var}_{\log(1+\tau^F_{ni})}(\tilde{\mathbf{T}}_{rt},\cdot)}{\partial \tilde{\mathbf{T}}_{rt}} \\
&\quad + \sigma_n \sum_{F\in\{K,L,M\}} \alpha_{Fn} \frac{\partial\, \text{cov}_{\log(1-\tau^Y_{ni}),\log(1+\tau^F_{ni})}(\tilde{\mathbf{T}}_{rt},\cdot)}{\partial \tilde{\mathbf{T}}_{rt}} \\
&\quad - (\sigma_n - 1) \sum_{F\in\{K,L,M\}} \sum_{F'\neq F} \alpha_{Fn}\alpha_{F'n} \frac{\partial\, \text{cov}_{\log(1+\tau^F_{ni}),\log(1+\tau^{F'}_{ni})}(\tilde{\mathbf{T}}_{rt},\cdot)}{\partial \tilde{\mathbf{T}}_{rt}}
\end{aligned}
\tag{10}
$$

Proof. See Appendix ■

The decomposition shows that the first-order effect of climate conditions on aggregate TFP can be captured entirely through the effect on technology and the effect on inefficiency losses through misallocation. This proposition provides theoretical foundations to understand the different channels through which climate conditions may result in aggregate losses and a practical framework for quantitatively measuring these changes.

Measurement Implications. All the structural moments presented in equation (10) are measurable from firm-level panel data. They can be estimated using standard approaches in the literature.

The composite productivity term ($B_{ni}(\tilde{\mathbf{T}}_{rt},\cdot)\left(A_{ni}(\tilde{\mathbf{T}}_{rt},\cdot)\right)^{\sigma_n-1}$) can be estimated via simple Solow residuals (as in Bils, Klenow, and Ruane (2021) and Asker, Collard-Wexler, and Loecker (2014)), or via production function estimation using methods such as Levinsohn and Petrin (2003) and Ackerberg, Caves, and Frazer (2015), coupled with the assumed structure of CES demand. Output distortions, often regarded as markups, can be estimated through the control function approach as in De Loecker and Warzynski (2012), or from the profit accounting approach or user cost approach as employed by Baqaee and Farhi (2019). Following the standard approach by Hsieh and Klenow (2009), Bau and Matray (2023) and Sraer and Thesmar (2023), firm-level input distortions can be easily measured by computing the marginal revenue product of factors (MRPF), which is proportional to $\frac{\text{revenue}}{\text{factor quantity}}$ under Cobb- Douglas production function.

Aggregating these statistics into the relevant first and second moments in Equation (10) at the region-sector-year level, we can then follow the standard approach in the climate econometrics literature to estimate the effect of temperature/precipitation shocks (e.g., Deschênes and Greenstone 2011; Dell, Jones, and Olken 2012) such that the causal elasticities of temperature on these structural moments, $\frac{\partial \textbf{Moments}_{nt}}{\partial \tilde{\mathbf{T}}_{rt}}$, can be identified.

Data Requirements. Our approach is fairly general but requires very detailed firm-level panels covering variables, including sales, capital stock, number of employees, wages, and intermediate inputs, across geographical locations featuring different long- and short-run climate conditions (as sources of variations). Compiling such a dataset requires a trade-off between variable coverage and data representativeness, as more than one-third of firm-year observations in most firm-level panel datasets are missing at least one of the variables listed here [7]. Therefore, we focus on a special case where only capital wedges are present, for which only data on revenue and fixed assets are needed in the sample, ensuring a wide data availability across geographical regions and representativeness of firms within each region-sector.

Special Case: only capital wedges are present. For expositional clarity and considerations on data representativeness, we now consider a simple case where only capital wedges are present. This is the benchmark case in David and Venkateswaran (2019), Sraer and Thesmar (2023), and Asker, Collard-Wexler, and Loecker (2014), with a view that capital is more of a dynamic input than labor or material. Moreover, the dispersion of capital distortions is also measured to be larger than that of labor (Gorodnichenko et al. 2018) as they cannot be adjusted easily after the realization of shocks. How capital misallocation is affected by climate conditions will be the main focus of empirical analysis throughout the paper. However, we will revisit the general case featuring various channels of misallocation in the Appendix.

When the capital wedge is the only source of distortions in the economy, within region-sector n, the MRPK of each firm i satisfies that:

$$\text{MRPK}_{nit} = \alpha_{Kn} \frac{P_{it} Y_{it}}{K_{it}} \propto (1 + \tau^K_{nit}) R_{nt},$$

which implies that

$$\text{var}(\log(1 + \tau_{nit})) = \text{var}(mrpk_{nit}) = \text{var}\left(\log\left(\frac{P_{it} Y_{it}}{K_{it}}\right)\right).$$

7. This is particularly true in Orbis, which is detailed in Appendix XXX.

The identity shows that the cross-sectional variance of (log) capital distortions across firms is identical to the dispersion of (log) MRPK, which can be computed via the variance of log sales over capital stock given the Cobb-Douglas technologies. Now, the effect of climate conditions on aggregate TFP will be simplified into:

$$\frac{\partial \log TFP_n(\tilde{\mathbf{T}}_{rt},\cdot)}{\partial \tilde{\mathbf{T}}_{rt}} = \frac{1}{\sigma_n - 1}\frac{\partial \log\left(\int B_{ni}(\tilde{\mathbf{T}}_{rt},\cdot)\left(A_{ni}(\tilde{\mathbf{T}}_{rt},\cdot)\right)^{\sigma_n-1} di\right)}{\partial \tilde{\mathbf{T}}_{rt}} - \frac{\alpha_{Kn} + \alpha_{Kn}^2(\sigma_n - 1)}{2}\frac{\partial\, \mathrm{var}_{mrpk,n}(\tilde{\mathbf{T}}_{rt},\cdot)}{\partial \tilde{\mathbf{T}}_{rt}}, \tag{11}$$

such that the (first-order) cost of climate-induced misallocation would be reduced to the estimation of elasticity $\frac{\partial\, \mathrm{var}_{mrpk_{ni}}(\tilde{\mathbf{T}}_{rt},\cdot)}{\partial \tilde{\mathbf{T}}_{rt}}$.

In theory, the derivatives of our structural objects with respect to climate conditions are globally well-defined and could vary with various histories of climate and economic conditions. However, in practice, it is preferable to think of them as "reduced form," which means that they can only be well estimated with respect to observed equilibrium allocations and are not necessarily invariant to the evolving climate conditions in the long run. For example, these first-order effects could increase with worsening global warming or decrease with gradual adaptation. We will address this explicitly in section 4.3 to capture the effect of long-run climate conditions and economic development.

3 Data (To be finished)

3.1 Global Firm-level Microdata

We compile an extensive global sample of microdata from both developed and developing economies. This compilation includes country-specific firm-level data from China, India, and 30 European countries, where the two developing countries form X% of world GDP. Each dataset has been widely employed in the literature. They vary regarding the periods they cover and the methods used for sampling producers. The firm-level panels for China and India were obtained from government-conducted surveys, and the data for the 30 European countries were from Bureau van Dijk's (BvD) Orbis database. For a comprehensive list of countries, years, and data sources, see Appendix XX, and refer to Appendix XX for additional details on data construction. Table X[8] summarizes the main features of the various datasets. Below, we provide a brief overview of the various datasets; more details and discussions are deferred to Appendix X.

BvD Orbis. Our data for European countries comes from the ORBIS dataset, which offers firm-level data for numerous countries globally. This data originates from administrative records collected at the firm level, primarily by each country's local Chambers of Commerce. A significant advantage of focusing on European countries with ORBIS is that company reporting is regulatory, even for small private firms.

8. Need a summary table here later.

ORBIS is distinguished by its comprehensive financial accounting information, which includes detailed and harmonized data from balance sheets, income statements, and profit and loss accounts of firms. Approximately 99 percent of the companies included are private entities, a significant differentiation from other datasets commonly used in finance research, such as Compustat for the United States, Compustat Global, and Worldscope, which predominantly contain information on large, publicly listed companies.

To clean and organize the ORBIS dataset, we follow Kalemli-Ozcan et al. (2015), Gopinath et al. (2017), and Nath (2023). Our analysis classifies these firms into eight major industry divisions with the U.S. Standard Industrial Classification (USSIC) code provided in the dataset. The industry included are: To Be Added

China. The annual firm-level data for China is derived from surveys conducted by the National Bureau of Statistics (NBS) in China. These surveys encompass all industrial firms with annual sales exceeding nominal CNY X million (approximately USD X million) from 1998 to 2011. Such firms are commonly referred to as "above scale" industrial firms[9]. The NBS data includes sectors such as mining, manufacturing, and public utilities, with manufacturing constituting X% of the total observations in the dataset. In processing the NBS data, we follow the methodology outlined in Zhang et al. (2018). Each firm in the dataset is categorized using a four-digit Chinese Industry Classification (CIC) code. This classification system is analogous to the USSIC code. Our final sample uses the 1-digit industry division to classify these firms.

India ASI. To Be Added.

3.2 Weather and Forecast Data

Climate. For climate data, we use the land component of the European ReAnalysis, known as ERA5-Land (Sabater 2019), produced by the European Centre for Medium-Range Weather Forecasts (ECMWF). ERA5-Land is a reanalysis dataset that combines historical observations with models to create a consistent time series of various climate variables. A main advantage of ERA5-Land is its enhanced temporal and horizontal resolution. It provides hourly data on surface variables at a spatial resolution of 0.1°longitude $\times$ 0.1°latitude (approximately 9 km), covering the entire world. This high resolution allows for a clearer depiction of the spatial patterns of surface temperature between neighboring locations.

Our analysis uses variables of air temperature at 2 meters above the land surface and total precipitation. We use binned daily average temperatures for our main specifications to effectively capture the non-linear relationship between the outcome variable and weather conditions. We bin daily temperature every 5°C from -5°C to 30°C. Each temperature bin counts the number of days in a year when the daily average temperature falls within specific temperature ranges. The daily average temperature is the simple geometric average of the maximum and minimum temperatures. The daily maximum temperature is identified by the highest value among the hourly temperatures, and the daily minimum temperature is the lowest recorded

9. According to the 2004 census of manufacturing firms by the NBS, these above-scale firms account for over X% of the total output.

value.

The use of daily temperature bins in our analysis better conceptualizes climate. Because climate change represents a long-term shift in weather patterns, the year-to-year variation in the whole temperature distribution offers a more accurate depiction of climate change than merely examining year-to-year variations in mean temperature. A key feature of climate change is the increased frequency of extreme heat events (Oudin Åström et al. 2013; Christidis, Mitchell, and Stott 2023), therefore the increase in the number of extreme hot bins, indicative of a rightward shift in the tail of the weather distribution, captures the idea of global warming more accurately.

We also collect historical temperature with a spatial resolution of 1°x 1°latitude-longitude from the Berkeley Earth Surface Temperature (BEST) dataset (Rohde et al. 2013). This is to construct our forecast error variables, aligning with the forecast data, gridded in 1°x 1°latitude-longitude cells. BEST interpolates observational data across a global grid, integrating approximately 39,000 land station records. This dataset covers about 95% of the Earth's surface in 1960, expanding to 99.9% by 2015. All weather data are aggregated using area-weighting methods.

Figure 1: Frequency of Extreme Hot Days in Europe

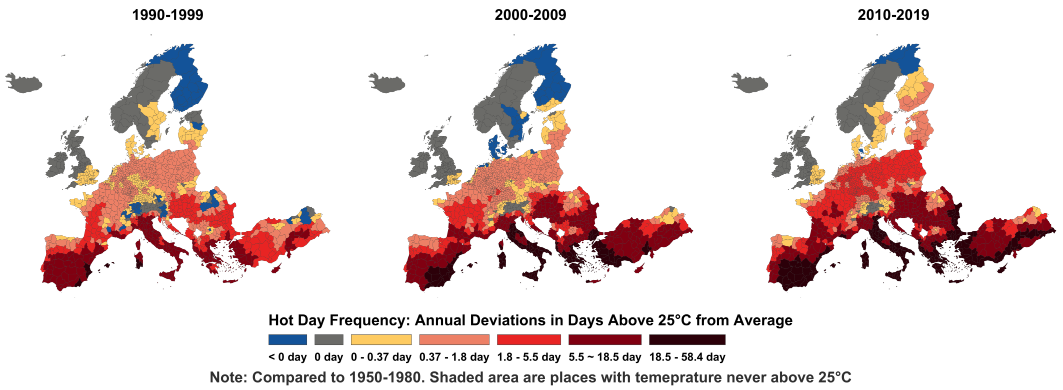

Notes: Figure to be changed with pixel-fashion ERA5 and BE data + weather / forecast summary statistics table.

Forecast. For weather forecast data, we collect the long-range (seasonal) forecast from ECMWF (Copernicus Climate Change Service and Climate Data Store 2018), which provides information about atmospheric and oceanic conditions up to seven months into the future. The forecast data have a spatial resolution of 1-degree longitude by 1-degree latitude. From 1981 to 2016, the forecast values were hindcasts generated with a 25-member ensemble. Starting in 2017, they are forecasts produced monthly with a 51-member ensemble. These ensembles are run on the first day of each month, providing forecasts for up to seven months ahead.

We collect forecast daily maximum 2m temperature from the first day of each month from January to December with forecasts up to 30 days measured in 724 lead-hours.

The daily forecast error is calculated as error $:= \mathrm{T}_{max} - \mathrm{F}_{max}$, where F represents the forecast and T the actual weather. We then compute the monthly mean squared forecast error (MSFE), using the formula $MSFE_m = \frac{1}{n}\sum_{i=1}^{n}\left(\mathrm{T}_{max,i} - \mathrm{F}_{max,i}\right)^2$, where n denotes the number of days in the month. We further aggregate monthly forecast error to seasonal forecast in the empirical analysis.

4 Estimating the Misallocation Effect of Climate Change

- Estimation Equation
- Explain variables
- Explain Parameters
- Interpret results
- Robustness

4.1 Identification of the Causal Elasticities on Misallocaton

We now estimate the first-order causal elasticities on capital misallocation $\frac{\partial \operatorname{var}_{mrpk_{ni}}(\tilde{\mathbf{T}}_{rt},\cdot)}{\partial \tilde{\mathbf{T}}_{rt}}$. Note that for each region-sector $n = (r, s)$, a Taylor expansion around the observed steady state $(\overline{\operatorname{var}_{mrpk_{(s,r)i}}}, \overline{\tilde{\mathbf{T}}_r}, \overline{\tilde{\mathbf{X}}_{s,r}})$ can be written as

$$\begin{aligned}\operatorname{var}_{mrpk_{(s,r)i}}(\tilde{\mathbf{T}}_{r,t}, \tilde{\mathbf{X}}_{s,r,t}) &= \overline{\operatorname{var}_{mrpk_{(s,r)i}}} + \boldsymbol{\lambda}^{s,r}_{\sigma^2_{mrpk}} \cdot (\tilde{\mathbf{T}}_{r,t} - \overline{\tilde{\mathbf{T}}_r}) + \boldsymbol{\delta}^{s,r}_{\sigma^2_{mrpk}} \cdot (\tilde{\mathbf{X}}_{s,r,t} - \overline{\tilde{\mathbf{X}}_{s,r}}) + H.O.T. \\ &\approx \boldsymbol{\lambda}^{s,r}_{\sigma^2_{mrpk}} \cdot \tilde{\mathbf{T}}_{r,t} + \boldsymbol{\delta}^{s,r}_{\sigma^2_{mrpk}} \cdot \tilde{\mathbf{X}}_{s,r,t} + \eta_{s,r},\end{aligned} \tag{12}$$

where $\eta_{s,r}$ is a sector-region specific constant. For our benchmark exercise, we first estimate the average causal elasticity $\boldsymbol{\lambda}_{\sigma^2_{mrpk}} = \mathbb{E}[\boldsymbol{\lambda}^{s,r}_{\sigma^2_{mrpk}}]$ across all climates and sectors. We will revisit the nature of heterogeneity across climates and sectors in Section 4.3 and C.1.

We define current climate conditions, $\mathbf{T}_t$, in terms of temperature bins, following the approach by Carleton et al. (2022), Deschênes and Greenstone (2011), and Nath (2023). These bins, spanning the vector $\mathbf{T}_t = \{\text{Tbin}^{<-5°C}_{r,t}, \text{Tbin}^{-5\sim0°C}_{r,t}, \text{Tbin}^{0\sim5°C}_{r,t}, \text{Tbin}^{5\sim10°C}_{r,t}, \text{Tbin}^{10\sim15°C}_{r,t}, \text{Tbin}^{15\sim20°C}_{r,t}, \text{Tbin}^{20\sim25°C}_{r,t}, \text{Tbin}^{25\sim30°C}_{r,t}, \text{Tbin}^{>30°C}_{r,t}\}$, capture the number of days within specific temperature ranges for region r in year t. Structured in 5-degree Celsius increments, these bins cover a broad spectrum of temperature variations, including extreme heat and cold. Thus, as noted in Deschênes and Greenstone (2011), using daily temperature data enables us to capture weather's nonlinear effects using linear regression models.

To estimate the causal effect of temperature on MRPK dispersion (i.e., misallocation), we follow the standard approach in Deschênes and Greenstone (2011) and Zhang et al. (2018) to exploit the inter-annual variation in the distribution of daily temperatures through the following panel regression:

$$\operatorname{var}_{mrpk_{(s,r),t}} = \sum_{b \in B/(5\sim10°C)} \lambda^b_{\sigma^2_{mrpk}} \times \text{Tbin}^b_{r,t} + \boldsymbol{\delta}_{\sigma^2_{mrpk}} \mathbf{X}_{s,r,t} + \alpha_{c(r),t} + \eta_{s,r} + \varepsilon_{r,s,t}, \tag{13}$$

where $\eta_{s,r}$ is the region-sector fixed effects, accounting for the unvarying attributes of MRPK dispersion specific to each region-sector pair over time, consistent with the formulation in Equation 12. $\alpha_{c(r),t}$ is the country-by-year fixed effects, capturing the aggregate shocks to the country c that region r resides in. Standard errors are clustered at the region level to account for both serial and spatial correlations between all sectors across all years within each region (NUTS3 in Europe, province in China, first-level administrative divisions in India).

$\lambda^b_{\sigma^2_{mrpk}}$ are coefficients measuring the causal effect of one additional day in temperature bin b on contemporaneous MRPK dispersion. Each $\text{Tbin}^b_{r,t}$ indicates the number of days whose average temperature falls within a specific range $b \in B$, where B is the set of ranges defined in 5-degree Celsius increments. Since the total number of days in a year always equals 365, we employ the temperature bin ranging from 0°C to 5°C as the reference category, meaning that the coefficient for this category is normalized to zero.

$\mathbf{X}_{s,r,t}$ is a vector of logged control variables at the region-sector-year level, including the total number of observed firms, average firm-level sales, and average MRPK[10]. The first two controls for the observed size and region-sector-level business cycle fluctuations. By controlling for the average (log)MRPK across firms at the region-sector-year level, we aim to demonstrate that the observed dispersion in MRPK is not primarily driven by the mechanisms through which temperature influences the average MRPK[11].

4.2 Average Effects of Temperature on Capital Misallocation

The estimates across different specifications of equation 13 are shown in Table F.2. Figure 2 plots our baseline estimates of the effects of heat exposure on annual MRPK dispersion and the implied TFP loss, as determined from the estimation of equation 13[12]. Specifically, Figure 2a plots the regression coefficients $\hat{\lambda}^b_{\sigma^2_{mrpk}}$ for all the bin b. Each $\hat{\lambda}^b_{\sigma^2_{mrpk}}$ quantifies the estimated impact of an additional day in temperature bin b on MRPK dispersion, compared to a day within the 5°C - 10°C range. To facilitate interpretation, in Figure 2b, we translate the estimates $\hat{\lambda}^b_{\sigma^2_{mrpk}}$ into the marginal effect on aggregate TFP through the misallocation channel using $-\frac{\alpha_{Kn}+\alpha^2_{Kn}(\sigma_n-1)}{2}\hat{\lambda}^b_{\sigma^2_{mrpk}}$ from equation 11 under the choice of well-established conservative choice of $\alpha_{Kn} = 0.175$ and $\sigma_n = 4$ across all n [13].

The estimated coefficients reveal that MRPK dispersion and the inferred TFP loss from temperature-induced misallocation peak at the most extreme temperatures, both coldest and hottest. This observed U-shape pattern between MRPK dispersion and temperature can also be translated into an inverted U-shape pattern between TFP and temperature, which is well known in the climate econometrics literature (Burke, Hsiang, and Miguel 2015; Nath 2023).

For temperatures above 25°C and below -5°C, the effects on MRPK dispersion are both economically and statistically significant at 1% level. Specifically, the point estimates indicate that substituting a day in the 5-10°C range with a day exceeding 30°C results in an increase of 0.4 log points in MRPK dispersion, translating to a decrease of 0.052% in annual aggregate

10. We exclude these controls in our preferred specification as they may block a potential pathway for affecting dispersion, although adding these controls have very little effect on our estimates.

11. This control allows us to isolate the specific impact of temperature on MRPK dispersion, independent of its effects on the average level of MRPK, as identified by Caggese et al. (2023). Controlling for average MRPK also reflects the average financial constraints across firms.

12. We later show graphs plotting both MRPK dispersion and implied TFP loss in the same graph.

13. For the elasticity of substitution, we choose $\sigma_n = 4$ as in Bils, Klenow, and Ruane (2021). For rescaled labor share $\alpha_n = 0.175$, we pick the valued added share of capital 0.35, multiplied by 0.5, a commonly-used value for VA share of gross output (e.g. David and Venkateswaran 2019).

Figure 2: Estimated impact of daily temperature shocks on annual MRPK dispersion and implied TFP loss

(a) Impact on MRPK dispersion (b) Impact on TFP loss

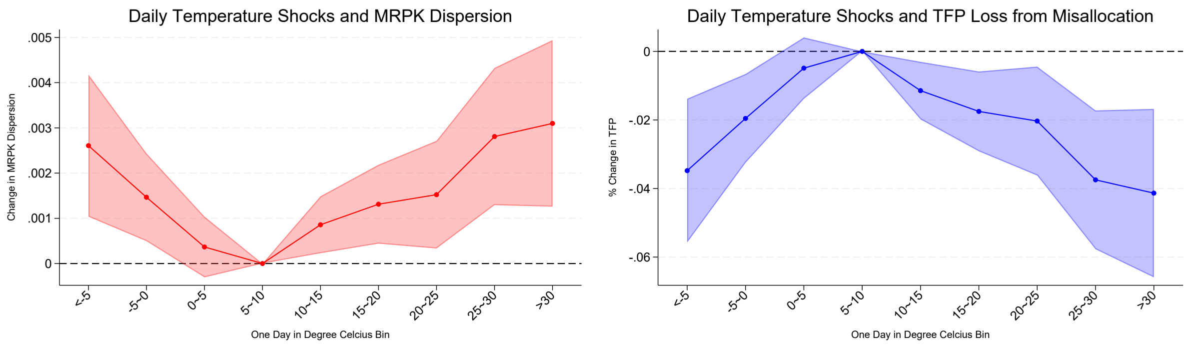

Notes: This figure shows the aggregate impact linking annual MRPK dispersion and TFP loss to average daily temperatures. This is derived by applying equation 13 to the variance in MRPK and the calculated TFP loss due to misallocation. The formula for computing TFP loss from misallocation is $-\frac{\alpha_{Kn}+\alpha_{Kn}^2(\sigma_n-1)}{2}\hat{\lambda}^b_{\sigma^2_{mrpk}}$. The estimation is normalized by setting the range of 5°C - 10°C as the reference category. Therefore, each $\lambda^b_{\sigma^2_{mrpk}}$ represents the estimated effect of an additional day in temperature bin b on annual MRPK dispersion or TFP loss, relative to a day with temperatures between 5°C - 10°C. The figure also includes the 90% confidence interval for these estimates where standard errors are clustered at the region level.

TFP due to capital misallocation. On the cold end, we find that an additional day colder than -5°C in a year leads to an approximate 0.3 log points increase in annual MRPK dispersion and 0.037% loss in annual TFP.

Robustness. Table F.2 presents results of estimates of equation 13 with different specifications of fixed effects, inclusions of control variables, and various weighting methods. Columns 1 and 6 report the baseline estimates and inferred TFP loss that was used to create Figure 2. Columns 2 - 5 provide robustness checks. We introduce country-sector-year fixed effects instead of country-year fixed effects in column 2, absorbing all unobserved country and year-specific, region-invariant factors affecting MRPK dispersion in each sector. Column 3 adds control variables, including total number of observed firms, average firm-level sales, and average level of MRPK across firms in a region-sector-year, all in logarithmic form. Columns 4 and 5 provide two weighting methods by weighting observations by the number of firms and average sales in the region-sector pair, respectively, which ensure that the region-sector with more firms or higher average sales receives more weight. The objective is to assess whether assigning greater influence to observations with a larger firm count or higher sales affects the outcomes of our analysis. The U-shaped pattern, peaking at extreme temperatures, persists in the coefficients, and our results remain robust under various specifications.

Comparison with the Technology Channel. To compare the relative contribution of the two channels to understand which channel might be the primary driver of aggregate productivity, we run a similar regression as in Equation 13 but with efficient TFP[14] as the dependent variable.

14. Move this footnote to main paperBased on our accounting framework, we measure efficient TFP as $\log TFP^E_{nt} = \frac{1}{\sigma_n-1}\log \mathbb{E}[B_{nit}A_{nit}^{\sigma_n-1}]$, under the assumption that capital distortions are the only source of misallocation in the economy and the measure of firms within each region-sector is constant over time. Here the va-

Figure 3 plots the TFP loss from temperature shocks of both channels under baseline specifications. As temperatures deviate from reference levels, the impact on TFP becomes increasingly negative for both channels. Two channels have quantitatively similar effects in cold days below the 5° C range. However, for hotter temperatures exceeding 10°C, the misallocation channel appears to have a stronger effect on aggregate productivity. Beyond this temperature range, the change in TFP from the misallocation channel exhibits a sharp decrease, whereas the change in TFP attributable to the technology channel begins to show ambiguous effects. To be concrete, the technology channel contributes to 0.004% of TFP Loss in a 25-30°C day and 0.04% in an above 30°C day. In comparison, the misallocation channel contributes to 0.045% of TFP Loss in a 25-30°C day and 0.052% in an above 30°C day, much larger than the technology channel. The comparison between the two channels reveals that the effect of temperatures on "technology": physical productivity and preferences are less prevalent than the large impact on the (ex-post) input allocation "mistakes" that firms make that reduce allocative efficiency. This argument is especially pertinent for most developed countries.

Table F.3 presents the detailed estimation results under different panel specifications. Taking stock across various specifications, we conclude that, on average, the misallocation channel contributes to at least half of the climate-related decline in region-sectoral aggregate productivity[15].

4.3 Heterogeneous Effect by Climate and Development

Our benchmark specification in equation 13 captures the average effect of temperature on capital misallocation $\mathbb{E}[\boldsymbol{\lambda}^{s,r}_{\sigma^2_{mrpk}}]$. However, it is not immediately clear if a hot day would consistently cause more or less misallocation in regions that are already warm or economically thriving. The ambiguity arises from two potentially counteracting factors. On the one hand, heat-sensitive firms in warmer climates might be more motivated to adapt to weather shocks and reduce the damage. On the other hand, the marginal effect of high temperatures might be more severe due to the inherent vulnerability of firms in already hot climates. This is suggested by structural models showing convex temperature damage, and the observed non-linear effects in empirical studies like Burke, Hsiang, and Miguel (2015). Similarly, in regions with higher income levels, while firms may possess greater resources for adaptation to heat shocks, these economies often have highly specialized productions and support many active small firms.

riety effect on TFP via entry/exit is muted by assuming a constant mass of firms in each region-sector across the observed sample. This assumption is because we could not credibly infer the variety effect as there might be selection from firms' financial reporting practices in any given region-sector across years. $B_{nit}^{\frac{1}{\sigma_n-1}} A_{nit}$ is the firm-level "productivity" which broadly refers to the mix of supply and demand forces, measured by $B_{nit}^{\frac{1}{\sigma_n-1}} A_{nit} = \frac{(P_{nit}Y_{nit})^{\frac{\sigma_n-1}{\sigma_n}}}{K_{nit}^{\alpha_{Kn}} (L^*_{nit})^{\alpha_{Ln}} (M^*_{nit})^{\alpha_{Mn}}}$ as in Bils, Klenow, and Ruane (2021) except that we use the efficient level of labor L^*_{nit} and material M^*_{nit} (calculated from equation (6)) to compute productivity for each firm to be consistent with our accounting in which we assume there are no labor and material distortions.

15. Of course, the comparison of the two channels should be interpreted with caution in the sense that the variables are computed under the assumption of CES aggregator and the existence of only capital-related distortions, although these assumptions are prevalent in the misallocation literature. The estimated effect could be somewhat different if one adopts a different form of aggregator and alternative assumptions regarding the distortion.For example, Baqaee and Farhi (2019) show that the joint distribution of productivity and wedges (or markups) could matter for productivity aggregation in more general contexts.

Figure 3: Technology Channel vs. Misallocation Channel

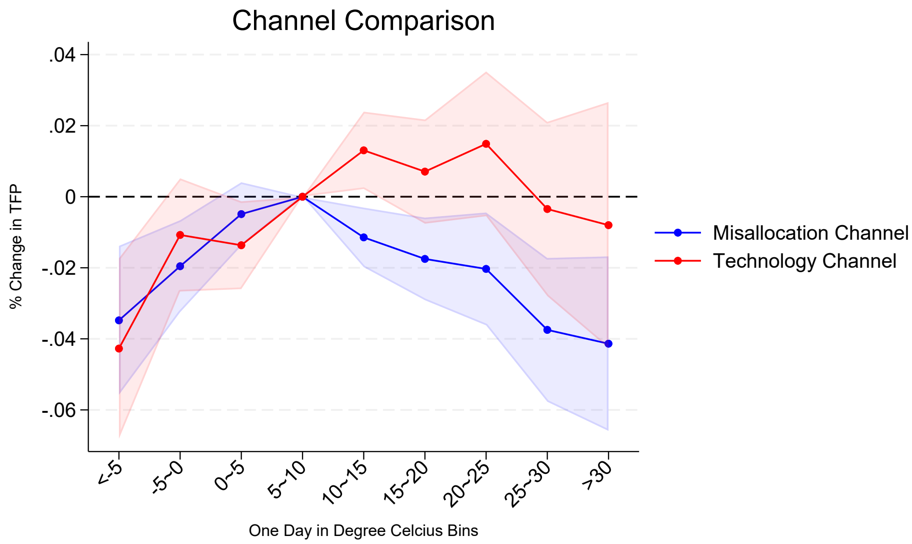

Notes: Graph plots the effects of daily mean temperature bins on TFP loss, decomposed into misallocation and technology channel. Overall, the effect of the technology channel remains ambiguous. The shaded area are 90% confidence interval.

These smaller enterprises may exhibit a wide array of temperature sensitivities, leading to heterogeneous responses to climate conditions, which we later show in Section 5a that dispersion in firm sizes contributes to the MRPK dispersion.

Therefore, to more precisely account for the climate and income heterogeneity across regions, we follow the approach of Carleton et al. (2022) and Nath (2023) by interacting the long-term annual average temperature of region r and country-level annual GDP per capita with each temperature bin. This approach allows us to capture how climate and income jointly influence the effects of temperature variations on capital misallocation. The modified regression model is formulated as follows:

$$\begin{aligned}\sigma^2_{mrpk_{s,r,t}} = &\sum_{b \in B_{/(5\sim10^\circ C)}} \lambda^b_{\sigma^2_{mrpk}} \times \text{Tbin}^b_{r,t} + \sum_{b \in B_{/(5\sim10^\circ C)}} \lambda^{b,\bar{T}}_{\sigma^2_{mrpk}} \times \text{Tbin}^b_{r,t} \times \overline{T}_r \\ &+ \sum_{b \in B_{/(5\sim10^\circ C)}} \lambda_{\text{GDP}_{pc}} \times \text{Tbin}^b_{r,t} \times \ln GDP_{c,t} + \boldsymbol{\delta}_{\sigma^2_{mrpk}} \times \tilde{\mathbf{X}}_{s,r,t} + \alpha_{c,t} + \eta_{s,r} + \varepsilon_{s,r,t},\end{aligned} \tag{14}$$

where $\overline{T}_r$ represents the long-run annual average temperature for region r. The coefficients $\lambda^{b,\bar{T}}_{\sigma^2_{mrpk}}$ and $\lambda_{\text{GDP}_{pc}}$ quantify how the impact of temperature on MRPK dispersion varies across regions with different productivity levels and climate[16].

Figure 4 presents the results from estimating Equation 14, displaying the impact of temperature on MRPK dispersion and equivalent TFP loss due to capital misallocation across three income and four climates levels, representative of our sample distribution. The left y-axis indicates changes in MRPK dispersion, while the right y-axis shows the implied TFP loss sug-

16. Interacting temperature bins with the region's long-term average temperature allows us to analyze how an exceptionally hot year affects areas with varying baseline climates. Similarly, by interacting temperature bins with a country's annual per capita income, we evaluate how the same heat shock impacts developed and developing economies differently.

gested by the estimates. Figure 4a report results from a pooled regression that includes China and India, along with European countries, and Figure 4b report results from restricting the sample to European countries alone.

Hotter regions suffer more from the misallocation Channel. Figure 4a shows that an extremely hot day (above 30°C) results in greater MRPK dispersion in regions with a hotter climate. In regions of comparable wealth, the adverse effects of extreme heat intensify as the regional climate becomes warmer, as observed when moving from the left column to the right. Heat shocks appear to decrease MRPK dispersion and reduce TFP loss in regions with a colder climate. In such scenarios, the heterogeneous impacts across different income groups are less discernible, as shown in the first column from the bottom up. The second and the third columns suggest that in regions with a climate ranging between 10 - 15°C, the impact of cold weather shocks on TFP loss is minimal, and hot weather shocks also show a less statistically significant effect on TFP loss.

Richer economies suffer more from the misallocation Channel. A second key finding is that wealthier economies are more adversely affected in the misallocation channel by extreme heat, which becomes even more evident when we narrow our focus to exclusively European countries. Specifically, for regions with a hotter climate, at 20°C, more advanced economies with a GDP per capita of $60,000 experience an increase in TFP loss of 0.4%, whereas less advanced economies with a GDP per capita of $30,000, only experience half of that impact, with a 0.2% increase in TFP loss.

These results show that the nature of the misallocation channel of climate change might be significantly different from other channels, such as labor productivity (Nath 2023) and mortality risk (Carleton et al. 2022). Previous empirical analysis showed that richer economies and hotter regions suffer much less from heat shocks in terms of labor productivity and mortality, suggesting that the effect of climate change might be somewhat adaptable[17]. However, the cost of climate change through the misallocation channel reveals a significant and contrasting pattern[18].

Replace the following two graphs with real Projection Results. To contextualize these findings, let us consider the example of Florida in the US, where the average temperature is around 20°C). Between 1981 and 2010, Florida typically experienced temperatures above 35°C for about seven days each year. Under moderate and high emissions scenarios, this frequency is expected to increase to 22 and 26 days per year, respectively, according to a report by Raimi,

17. Firstly, as a region becomes consistently hotter, workers are more adapted to the hotter climate and would not find a heat shock. Secondly, as an economy grows richer, it might suffer less. Both channels suggest that the cost of climate change might be lower in developed economies.

18. In Section 6, we identify some potential mechanisms that could help explain why hotter and richer regions suffer more from heat shocks. Specifically, we find that a positive temperature shock in hotter regions would increase TFP volatility, making firms more prone to input mistakes, while a hot temperature shock in cold regions might enjoy a slight decrease in TFP volatility. Moreover, a firm's adaptability to heat and cold shocks depends heavily on size. On the firm level, we show that smaller firms' MRPK is more sensitive to extreme temperatures than larger firms. Across region-sector pairs, we find that economies with larger size dispersion suffer more misallocation, which is consistent to the firm-level evidence. We find those region-sectors with large size dispersion are also those with higher incomes (i.e., more developed), consistent with Poschke (2018).

Keyes, and Kingdon (2020). When we apply our estimates of the costs due to misallocation to these projections, it implies a potential reduction in TFP by 4% in Florida, which is prominent among other channels of climate change (Need to cite the estimated loss from other channels in other papers). Further illustrating the heterogeneous impacts across different income levels, let us consider Singapore and Colombia, both with an annual average temperature of 27°C but vastly different per capita incomes of 82,807$ and 6,630$, respectively. Under the SSP5-8.5 scenario, as projected with CMIP6 obtained from *World Bank Climate Change Knowledge Portal* (2023), Singapore is expected to face an additional 30 days per year with temperatures exceeding 30°C at the end of the century, potentially leading to an 11% TFP loss. In contrast, Colombia is projected to experience an increase of 16 such days, translating to a 4% TFP loss[19].

These findings also suggest a range for optimal temperature, or "bliss point", of between 10 to 15°C, aligning with previous research in the field, such as the studies by Burke, Hsiang, and Miguel (2015) and Nath, Ramey, and Klenow (2023). This bliss point indicates an optimal temperature at which economic productivity is least affected. We come back to discuss the bliss point in Section 5.

19. It is also important to note that these estimates represent a conservative assessment, as they do not yet incorporate the effects of potential economic growth over this period.

Figure 4: MRPK Dispersion and TFP Loss Across Climates and Income

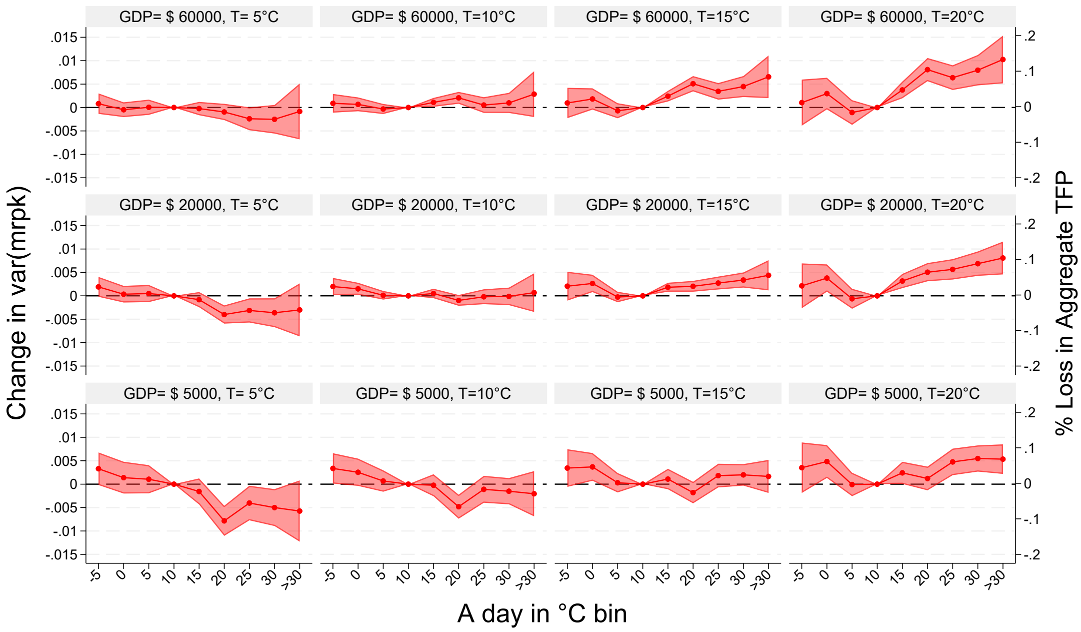

(a) Including China and India

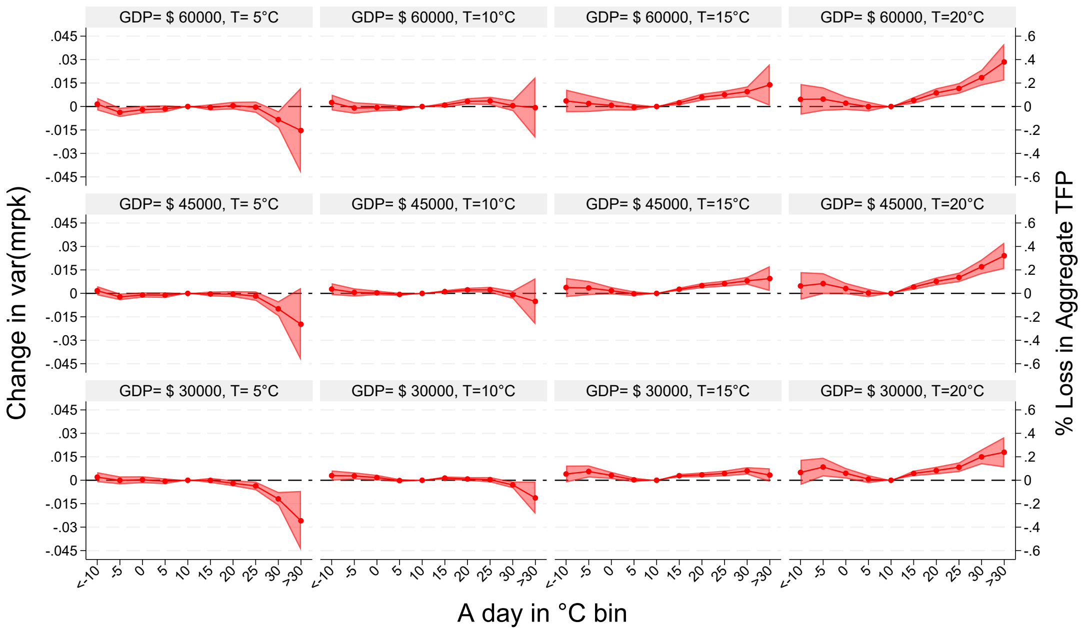

(b) Only European countries

Notes: The graphs plot the predicted effect of exposure to daily mean temperature bins on MRPK dispersion and TFP loss at varying levels of income and climates. These predicted effects are derived from the interacted panel regression specified in Equation 14. The graphs include 90% confidence intervals, and standard errors are clustered at the regional level. The left y-axis indicates changes in MRPK dispersion, and the right y-axis shows the calculated TFP loss. The plots can be interpreted as the effect of an additional day within a specific temperature range on the x-axis, compared to a day within the range of 5°C - 10°C. For example, in the top right cell of Figure 4b, which corresponds to a region-sector with a country GDP per capita of $60,000 and climate at 20°C, the results suggest that an additional day with temperatures exceeding 30°C in a year leads to a 0.4% increase in annual TFP loss for the region-sector. The reference temperature is at 5∼10°C, at the tick of 10°C.

5 A Firm Dynamics Model of Temperature Shocks and MRPK Dispersion

Misallocation affecting aggregate productivity features a second moment unexpected temperature shock in the model. We therefore propose a model with two sources of uncertainty: damage sensitivity from temperature and climate volatility from warming. Our model focuses on the dynamic investment decisions of firms in the context of climate conditions to understand the mechanisms through which climate shocks influence capital misallocation. This model incorporates factors such as firm-specific exposure to temperature, the uncertainty associated with climate conditions, and the unpredictability of resultant damages. These fundamental mechanisms lead to variations in the marginal products of capital—even when firms are subject to the same external climate conditions.

5.1 Setup

Similar to the accounting framework in Section 2, our model describes the action of firms and the aggregate economy within a region sector $n = (r, s)$. We suppress the label to avoid notation burdens.

Production and Demand. We begin by describing the production side of the economy. Each firm i produces differentiated products of quantity Y_{it} with Cobb-Douglas technology:

$$Y_{it} = \tilde{A}_{it} K_{it}^{\tilde{\alpha}_K} N_{it}^{\tilde{\alpha}_N}, \quad \tilde{\alpha}_K + \tilde{\alpha}_N = 1 \tag{15}$$

$\tilde{A}_{it}$ is the physical productivity, K_{it} is the capital input (which is dynamic) and N_{it} represents a composite of flexible inputs, referred to as "labor". The firm's product faces a constant elasticity downward-sloping demand curve with demand shifter B_{it}:

$$Y_{it} = B_{it} P_{it}^{-\sigma}.$$

Combing production and demand functions, we obtain the equilibrium revenue function of the form:

$$P_{it} Y_{it} = \hat{A}_{it} K_{it}^{\alpha_K} N_{it}^{\alpha_N} \tag{16}$$

where $\alpha_F = (1 - \frac{1}{\sigma})\tilde{\alpha_F}, \forall F \in \{K, N\}$ and $\hat{A}_{it} = B_{it}^{\frac{1}{\sigma}} \left(\tilde{A}_{it}\right)^{(1-\frac{1}{\sigma})}$ is the revenue-based productivity (TFPR). We will be referring to this simply as productivity.

Productivity and Heterogeneity in Heat Exposures. We now introduce how firms' productivity is heterogeneously impacted by temperature. Note that here, we allow the annual temperature to be a sufficient statistic for climate conditions for tractability (as in Dell, Jones, and Olken (2012) and Cruz and Rossi-Hansberg (2023)). We assume that firms' productivity can be linearly affected by temperature:

$$\hat{A}_{it} = \exp\left(\hat{\beta}_{it}(T_t - T^*)\right) \hat{Z}_{it}, \tag{17}$$

where T_t is the realized temperature at year t, T^* is an optimal temperature level for an average firm in the economy (in the sense that temperature would be irrelevant for all firms' production). We assume that each firm i's productivity changes linearly with temperature's deviation from average optimum, $T_t - T^*$, subject to the sensitivity $\hat{\beta}_{it}$. $\hat{Z}_{it}$ denotes firm-specific idiosyncratic productivity, which captures all the variations apart from the effect of temperature. The heterogeneity of $\hat{\beta}_{it}$ across firms reflects the composite effect of how both physical productivity and demand shifter are impacted by temperature.

One key element is allowing a firm i's temperature sensitivity $\hat{\beta}_{it}$, to be both firm-specific and time-varying. There are two sources of heterogeneity in a firm's exposure to temperature:

$$\hat{\beta}_{it} = \underbrace{\hat{\beta}_i}_{\substack{\text{Persistent}\\\text{sensitivity to}\\\text{temperature}}} + \underbrace{\hat{\xi}_{it}}_{\substack{\text{Idiosyncratic}\\\text{temperature}\\\text{damage}}}$$

1) The persistent sensitivity to temperature, $\hat{\beta}_i$, which is assumed to be observable and known to firms (e.g., a ski resort's $\hat{\beta}_i$ is negative, and the owner knows about it). We assume that $\hat{\beta}_i$ is distributed as $\hat{\beta}_i \sim \mathcal{N}\left(\bar{\hat{\beta}}, \sigma^2_{\hat{\beta}}\right)$ across firms, where $\sigma^2_{\hat{\beta}}$ measures the average heterogeneous exposure within a region-sector.

2) The idiosyncratic temperature damage sensitivity, $\hat{\xi}_{it}$, is i.i.d. across firm and time and cannot be predicted. It follows a normal distribution, $\hat{\xi}_{it} \sim \mathcal{N}\left(0, \sigma^2_{\hat{\xi}}\right)$, where $\sigma^2_{\hat{\xi}}$ measures the damage uncertainty within a region-sector.

Jointly, we model $\hat{\beta}_{it}$ in such ways to capture the idea that a firm would react to (realized and expected) temperature conditions according to their known knowledge of the firm's characteristics. However, they could not act optimally as there is always some unknown damage sensitivity to temperature every period.

We only allow the annual average temperature to be sufficient statistics for climate conditions here for tractability purposes. In a more general set-up in Appendix XXX, we allow sensitivity and temperature conditions to be vectors, $\boldsymbol{\beta}_i \mathbf{T}_t$, to capture the idea that some firms might suffer from both too cold and too hot temperature conditions.

Law of Motion for Productivity and Temperature. We assume (agents perceive that) temperature and (log) idiosyncratic productivity $\hat{z}_{it} = \log \hat{Z}_{it}$[20] follow an AR(1) process, with persistence ρ_T and ρ_z, respectively:

$$\begin{aligned} T_{t+1} &= \rho_T T_t + \eta^T_{t+1} + (1-\rho_T)\bar{T}, \\ \hat{z}_{it+1} &= \rho_z \hat{z}_{it} + \hat{\varepsilon}_{it+1}, \end{aligned} \tag{18}$$

where we assume that temperature oscillates around a local average $\bar{T}$. $\eta^T_{t+1} \sim \mathcal{N}\left(0, \sigma^2_\eta\right)$ is the temperature shock and the idiosyncratic productivity shocks $\hat{\varepsilon}_{it+1} \sim \mathcal{N}\left(0, \sigma^2_{\hat{\varepsilon}}\right)$ are independent across firms and time. At the firm level, uncertainty arises from three sources: 1) idiosyncratic weather damage sensitivity $\hat{\xi}_{it}$, normally distributed with variance $\sigma^2_{\hat{\xi}}$; 2) aggregate weather uncertainty with variance σ^2_η; and 3) idiosyncratic uncertainty, with variance $\sigma^2_{\hat{\varepsilon}}$.

20. We use lower case to denote variables in logs, except for temperature T_t.

We assume firms have full information regarding all realized shocks and hold rational expectations regarding the future states of the economy. We refer to the cross-sectional variance of unexpected firm-level TFP shocks as *TFP Volatility*, following Asker, Collard-Wexler, and Loecker (2014). TFP volatility in the model depends endogenously on temperature levels T_t and the temperature shocks η_t^T:

Lemma 1 *TFP Volatility,* $\mathrm{Var}(\hat{a}_{it} - \mathbb{E}_{t-1}[\hat{a}_{it}])$*, and can be written as:*

$$\mathrm{Var}(\hat{a}_{it} - \mathbb{E}_{t-1}[\hat{a}_{it}]) = (T_t - T^*)^2 \sigma_{\hat{\xi}}^2 + \hat{\eta}_t^{T\,2} \sigma_{\hat{\beta}}^2 + \sigma_{\hat{\varepsilon}}^2 \tag{19}$$

TFP Volatility reaches its minimum when the temperature reaches its optimum $T_t = T^*$*, and there is no unexpected change in temperature,* $\eta_t^T = 0$*.*

This lemma illustrates that TFP volatility is dependent on the regional climate. Suppose a region is too hot or cold compared to T_t^*. In that case, it will have a very volatile TFP shock due to the volatility of uncertain damage. We will test this empirically in Section 7.1.

Temperature and wages. Firms hire a composite of flexible inputs, "labor", on a period-by-period basis at a competitive wage, W_t. For simplicity in modeling the temperature-related supply- and demand-side frictions in the labor market (e.g., temperature-related disutility of work or temperature-induced loss of labor productivity), we assume the equilibrium wage is given by:

$$W_t = \overline{W} \exp\left(\chi(T_t - T^*)\right),$$

where the wage is a function of temperature (deviation from T^*) with constant elasticity χ, indicating the sensitivity of which wages respond to temperature[21].

Flexible Input Choice and Profits. Optimal choice of flexible inputs is made after capital inputs are allocated, and all shocks are realized. The static input choice solves

$$\max_{N_{it}} \exp\left(\hat{\beta}_{it}\left(T_t - T^*\right)\right) \hat{Z}_{it} K_{it}^{\alpha_K} N_{it}^{\alpha_N} - W_t N_{it},$$

and results in the operating profits Π_{it}, calculated as revenue minus labor costs, expressed as

$$\Pi_{it} = G A_{it} K_{it}^{\alpha} := G \exp\left(\beta_{it}(T_t - T^*) + z_{it}\right) K_{it}^{\alpha} \tag{20}$$

where $G := \overline{W}^{-\frac{\alpha_N}{1-\alpha_N}} \alpha_N^{\frac{\alpha_N}{1-\alpha_N}} (1 - \alpha_N)$, $z_{it} = \frac{1}{1-\alpha_N} \hat{z}_{it}$, and $\alpha = \frac{\alpha_K}{1-\alpha_N}$. We define capital profitability as $A_{it} := \exp\left(\beta_{it}(T_t - T^*) + z_{it}\right)$, where $\beta_{it} = \frac{\hat{\beta}_{it} - \chi\alpha_N}{1-\alpha_N}$ is the sensitivity of capital profitability to temperature, transformed from the firm's productivity's temperature sensitivity, $\hat{\beta}_{it}$, and the wage's temperature sensitivity, χ. α is the curvature of the profit function.

Dynamic Capital Investment. Capital is a dynamic input in the model and needs to be invested one period ahead before all shocks (including temperature) are realized. Thus, the

21. This assumption is commonly used in business cycle analysis. See Blanchard and Galí (2010), Alves et

investment problem can be formulated into the Bellman equations of the form:

$$V(T_t, Z_{it}, K_{it}) = \max_{K_{it+1}} \quad G \exp\left(\beta_{it}(T_t - T^*) + z_{it}\right) K_{it}^{\alpha} - K_{it+1} + (1-\delta)K_{it} + \frac{1}{1+r}\mathbb{E}_t\left[V\left(T_{t+1}, Z_{it+1}, K_{it+1}\right)\right],$$

where the firm exhibits no risk aversion nor adjustment costs in this simple model. $\frac{1}{1+r}$ is the discount factor. The optimal investment K_{it+1} solves the Euler equation:

$$1 = \underbrace{\frac{1}{1+r}}_{\text{Discount Factor}} \left(\underbrace{\alpha G K_{it+1}^{\alpha-1}\mathbb{E}_t\left[\exp\left(z_{it+1} + \beta_{it+1}(T_{t+1} - T^*)\right)\right]}_{\text{Expected Value of Marginal Profits of Capital}} + \underbrace{(1-\delta)}_{\substack{\text{Value of} \\ \text{Undepreciated Capital}}} \right). \tag{21}$$

Equation (21) shows that capital investment is increasing in the forecast of capital profitability, which in turn depends on the expectation of (1) idiosyncratic productivity z_{it+1}, (2) temperature sensitivity β_{it+1}, and (3) temperature T_{t+1}.

Solving the Euler Equation yields the firm's optimal investment policy as a function of expectations in logs (while ignoring higher-order risk-adjusted terms[22]):

$$\begin{aligned} k_{it+1} =& \frac{1}{1-\alpha}\mathbb{E}_t[a_{it+1}] + k_0 \\ =& \frac{1}{1-\alpha}\left(\frac{1}{1-\alpha_N}\mathbb{E}_t[\hat{a}_{it+1}] - \frac{\alpha_N}{1-\alpha_N}\mathbb{E}_t[w_{t+1} - \overline{w}]\right) + k_0 \\ =& \frac{1}{1-\alpha}\left(\frac{1}{1-\alpha_N}\left(\mathbb{E}_t[\hat{z}_{it+1}] + \mathbb{E}_t[\hat{\beta}_{it+1}(T_{t+1} - T^*)]\right) - \frac{\alpha_N \chi}{1-\alpha_N}\mathbb{E}_t[T_{t+1} - T^*]\right) + k_0, \end{aligned} \tag{22}$$

where $k_0 = \frac{1}{1-\alpha}\left(\log\left[\frac{\alpha G}{r+\delta}\right]\right)$ and lowercase denotes logs. Investment decisions are increasing in expected (revenue) productivity and decreasing in expected wages. Specifically, for a sufficiently heat-averse firm with $\hat{\beta}_i < \alpha_N \chi$ (say, a ski resort), a higher temperature forecast $\mathbb{E}_t[T_{t+1}]$ will lower its expected productivity $\mathbb{E}_t[\hat{a}_{it+1}]$ more than the change in expected wage $\mathbb{E}_t[w_{t+1}]$, which will result in a low-level of expected capital profitability $\mathbb{E}_t[a_{it+1}]$ and investment. In contrast, a heating-loving firm with more positive sensitivity to temperature, $\hat{\beta}_i > \alpha_N \chi$ (say, a water park), would even raise its investment due to the expected positive productivity shock[23] even when the expected temperature $\mathbb{E}_t[T_{t+1}]$ is high.

The expression in Equation 22 holds for more general expectation formation process and law of motion of temperature T_t, idiosyncratic sensitivity $\hat{\beta}_{it}$ and idiosyncratic productivity $\hat{z}_{it}$ with Gaussian innovations. Under our assumed AR(1) processes in Equations 18, the optimal investment decision follows that:

$$k_{it+1} = \frac{1}{1-\alpha}\left(\rho_z z_{it} + \beta_i(\rho_T T_t + (1-\rho_T)\bar{T} - T^*)\right) + k_0, \tag{23}$$

where the firm's capital choice rises with current productivity and either rises with current

al. (2020), and Flynn and Sastry (2023).

22. Full derivations including the risk-adjusted terms are presented in Online Appendix XXXXXX

23. Again, productivity here is revenue productivity, a combination of physical productivity and changes in pref-

temperature if the firm is heat-loving or declines with current temperature if the firm is heat-averse. All else equal, extremely heat-averse or extremely heat-loving firms would have more volatile capital investment patterns than those with little sensitivity to temperature $\beta_i \approx 0$. (Need to test this to put it here).

MRPK. Upon the realization of idiosyncratic productivity and temperature conditions, firms' labor choice is made and production takes place. From equation (20), realized marginal revenue product of capital ($MPRK_{it} := \alpha_K \frac{P_{it}Y_{it}}{K_{it}}$) [24] of firm i can be derived as (in logs):

$$mrpk_{it} = a_{it} + (\alpha - 1)k_{it} + \log(\alpha_K \bar{G})^{25} \tag{24}$$

Plugging in the policy function k_{it} as a function of past expectation, we write down find how $mrpk_{it}$ depends on the realization of shocks in the next proposition:

Proposition 4 *MRPK increases in the unexpected change in productivity:*

$$\begin{aligned} mrpk_{it} &= (a_{it} - \mathbb{E}_{it-1}[a_{it}]) + \log(r+\delta) \\ &= \frac{1}{1-\alpha_N}\left\{ (\hat{a}_{it} - \mathbb{E}_{it-1}[\hat{a}_{it}]) - \chi\alpha_N(T_t - \mathbb{E}_{t-1}[T_t]) \right\} + \log(r+\delta) \\ &= \frac{1}{1-\alpha_N}\left(\underbrace{\hat{\beta}_i \eta_t^T}_{\substack{\text{Unexpected}\\ \text{T Shock}\\ \text{on Productivity}}} + \underbrace{\hat{\xi}_{it}(T_t - T^*)}_{\substack{\text{Unexpected}\\ \text{Damage}\\ \text{Sensitivity}}} - \underbrace{\chi\alpha_N\eta_t^T}_{\substack{\text{Unexpected}\\ \text{T Shock}\\ \text{on Wage}}} + \hat{\varepsilon}_{it} \right\} + \log(r+\delta) \end{aligned} \tag{25}$$

On average, the MRPK of heat-averse firms with $\hat{\beta}_i < \chi\alpha_N$ will decrease with a positive temperature shock η_t^T; while the MRPK of cold-averse firms $\hat{\beta}_i > \chi\alpha_N$ will increase with a positive temperature shock.

Proof. See Appendix. ■

The first expression suggests that in the efficient benchmark where capital profitability is perfectly known at the time of investment, MRPK for all firms would be equalized to the user cost of capital. Otherwise, MRPK should increase with the forecast error of (revenue) productivity and decrease with the unexpected wage.

The last expression in Equation 25 reveals the key mechanism in the model. All firm's MRPK would change with (1) the unexpected temperature shock η_t^T due to their temperature sensitivity $\hat{\beta}_i$ and (2) with the level of temperature $T_t - T^*$ since part of their damage sensitivity $\hat{\xi}_{it}$ was unknown to them at the time of investment. Moreover, in a period with an unexpected heat shock, $\eta_t^T > 0$, the firms with relatively low MRPKs in the cross-section are those with (1) $\hat{\beta}_i < \chi\alpha_N$ (i.e. heat-averse) such that the productivity suffers unexpectedly more than other firms; (2) unexpected damage $\hat{\xi}_{it}(T_t - T^*) < 0$. Judging from ex-post, these firms invested too much capital beforehand, and the capital in those firms cannot be used as productively as those firms with $\hat{\beta}_i > \chi\alpha_N$ (cold-averse) or those experiencing experience an unexpectedly

erences

24. Note that the marginal revenue product of capital and the marginal profitability of capital are the same up to a transformation, which implies that their cross-sectional log dispersion should be the same.

less damage $\hat{\xi}_{it}(T_t - T^*) > 0$. This implies that temperature conditions will lead to dispersion in capital return and thus capital misallocation across firms, summarized by the following proposition, where we add back the notation for a region-sector pair $n = (r, s)$:

Proposition 5 *Within a region-sector pair $n = (r, s)$, the $mrpk$ dispersion across firms is increasing in TFP Volatility, $\mathrm{Var}(\hat{a}_{nit} - \mathbb{E}_{t-1}[\hat{a}_{nit}])$, and can be decomposed into:*

$$\begin{aligned}\sigma^2_{mrpk,(r,s),t} &= \left(\frac{1}{1-\alpha_N}\right)^2 \mathrm{Var}(\hat{a}_{nit} - \mathbb{E}_{t-1}[\hat{a}_{nit}]) \\ &= \left(\frac{1}{1-\alpha_N}\right)^2 \Bigg[\underbrace{(T_{r,t} - T^*)^2\sigma^2_{\xi,(r,s)}}_{\substack{\text{Damage Uncertainty}\\ \text{Channel}}} + \underbrace{{\eta^T_{r,t}}^2\sigma^2_{\beta,(r,s)}}_{\substack{\text{Climate Uncertainty}\\ \text{Channel}}} + \sigma^2_{\varepsilon,(r,s)}\Bigg]\end{aligned} \tag{26}$$

Within $n = (r, s)$, $mrpk$ dispersion is increasing in:

(1) squared deviation from optimal temperature, $(T_{r,t+1} - T^*)^2$,

(2) squared (unexpected) temperature shocks ${\eta^T_{r,t}}^2$.

As MRPK depends solely on the unexpected shocks on productivity and wages in the model, it follows naturally that MRPK dispersion scales with the dispersion in the unexpected shocks on productivity in the cross-section of firms. The higher the TFP volatility, the larger the dispersion of the input mistakes that would take place. Using our decomposition of TFP Volatility in equation (19), we find temperature variations contribute to misallocation through two channels: damage uncertainty and climate uncertainty.

(1) The damage uncertainty channel operates through that as all firms are facing some degree of unknown damage sensitivity $\hat{\xi}_{it}$, as the temperature deviates more from the "bliss point" T^*, firms who receive extreme realizations of $\hat{\xi}_{it}$ will get either larger unexpected damage or unexpected benefits. Productivity becomes harder to forecast, and more investment mistakes are made. The economy will thus have more misallocation as $(T_{r,t+1} - T^*)^2$ rises.

(2) The magnitude of the climate uncertainty channel relies on the size of unexpected temperature shocks. As different firms have heterogeneous sensitivity to these shocks, larger unexpected temperature shocks, either heat or cold, will make the return to investment of either cold-averse or heat-averse firms unexpectedly high while the other is unexpectedly low. Therefore, we will see an increasing level of capital misallocation with a more considerable unexpected temperature shock ${\eta^T_{r,t}}^2$.

Equation 26 also has predictions across region-sectors on how the average degree of misallocation in the region-sector depends on the average climate conditions and the distribution of the firm's weather-related characteristics:

Proposition 6 *Across region-sector pair $n = (r, s)$, Ceteris paribus, the steady-state $mrpk$ dispersion will be higher where:*

(1) average temperature deviates more from T^*, such that $(\bar{T}_r - T^*)^2$ is larger;

(2) temperature shocks are more unpredictable, such that $\sigma^2_{\eta,r}$ is larger;

(3) dispersion in persistent sensitivity $\sigma^2_{\beta,(s,r)}$ is larger;

(4) temperature damage uncertainty $\sigma^2_{\xi,(s,r)}$ is larger.

Proof. See Appendix. ■

The first two points explain how a region-sector's geographical locations might matter for capital misallocation. Regions experiencing extreme climates - either too hot or too cold - or those subject to volatile temperature conditions are prone to higher levels of capital misallocation. Additionally, the distribution of firms' characteristics is also pivotal: economies with greater damage uncertainty or larger heterogeneity of temperature sensitivity are likely to experience a higher degree of misallocation.

Specifically, notice the model suggests that the average level of temperature sensitivity $\overline{\hat{\beta}}_{(s,r)}$ in a region-sector does not matter for the degree of misallocation. This might explain why developed countries suffer more from temperature shocks via the misallocation channel. Although developed countries might feature a higher level of "heat preparedness" $\overline{\hat{\beta}}_{(s,r)}$, but might have a larger dispersion $\sigma^2_{\beta,(s,r)}$ due to the larger scope of specialized production and more extensive variety. Conversely, developing countries might feature more homogeneous production technique and most firms might not be unable to invest in adaptation, resulting in a relatively low dispersion of sensitivities.

TFP Loss from Misallocation. Similar to the aggregation exercise in the accounting framework, we formalize how temperature-induced misallocation affects region-sector aggregate TFP. In the Appendix, we show that the economy admits an aggregate production function of the form:

$$y_{nt} = a_{nt} + \tilde{\alpha}_K k_{nt} + \tilde{\alpha}_N n_{nt},$$

where the cost of misallocation can be expressed as the deviation from the level of TFP, a^*_{nt} when MRPKs are equalized across firms:

$$a_{nt} - a^*_{nt} = -\frac{1}{2}\frac{\alpha_K}{(1-\alpha_N)(1-\alpha_K-\alpha_N)}\sigma^2_{mrpk,nt} \tag{27}$$

This formula is reminiscent of equation (7) in the accounting framework and shows that the intuitions behind the cost of misallocation are similar in the partial equilibrium model.[26]

6 Firm-level Evidence: Heterogeneous Sensitivity, Temperature Shocks, and MRPK Divergence

We now provide direct evidence from firm-level data on how temperature shocks could lead to heterogeneous responses in the MRPK among firms with differing levels of temperature sensitivity[27], $\hat{\beta}_i$. As it is hard to directly measure $\hat{\beta}_i$ for each firm, we instead explore two possible

26. The model offers a simple combination of ingredients for us to capture the misallocation channel induced by climate conditions and is not catered to explain the total aggregate consequences of the volatility channel of temperature shocks in the economy. In particular, with the presence of the Oi-Hartman-Abel (OHA) effect in the model, an increase in temperature-induced productivity dispersion might actually lead to an increase in a^*_{nt}, creating an offset effect. This is a well-known result in Oi (1961), Hartman (1972) and Abel (1983). There are several ways to work around this, such as introducing Jensen's Inequality offset terms as in David and Zeke (2021), linear technology shocks (as opposed to log-linear) as in Fajgelbaum, Schaal, and Taschereau-Dumouchel (2017), or non-CES demand curve as in Carlsson, Clymo, and Joslin (2022), but these are beyond the scope of this paper.

27. This also serves to identify climate-induced misallocation directly using firm-level microdata without the log-

major factors contributing to this heterogeneity: the firm size and adaptability, particularly regarding air conditioning (AC) facilities. We examine whether the MRPKs of firms with different sizes and varying levels of adaptability (those equipped with AC-equipped versus those without) respond differently to the same temperature shocks.

It has been documented that larger firms are less sensitive to temperature shocks and can guard against extreme heat better than small firms (Ponticelli, Xu, and Zeume 2023), translating into a high level of $\hat{\beta}_i$ in the model Why size matters? ivan's comments page 39.

We test the key prediction by the model from Equation 25 (reproduced below). In the same region-sector pair, a more heat-averse firm (i.e. smaller $\hat{\beta}_i$) would have a lower MRPK from an unexpected positive temperature shock. As the temperature shock was not expected at the time of investment decisions, a more heat-averse firm would be seen to have made a bigger "investment mistake" as the return on the capital was unexpectedly low.

$$mrpk_{it} = \frac{1}{1-\alpha_N}\left(\underbrace{\hat{\beta}_i \eta_t^T}_{\substack{\text{Unexpected} \\ \text{T Shock} \\ \text{on Productivity}}} + \hat{\xi}_{it}(T_t - T^*) - \chi \alpha_N \eta_t^T + \hat{\varepsilon}_{it} \right) + \log(r+\delta)$$

6.1 Sources of β_i

We run the following regression as the empirical counterpart of the equation (25) to explore whether the two heat-averse indicator variables: firm sizes and No AC installment, lead to different responses of MRPK to temperature shocks:

$$\begin{aligned}\log(MRPK_{r,s,i,t}) = & \sum_{b \in B/\{5-10°C\}} \lambda_b \times \text{Tbin}_{r,t}^b \\ & + \sum_{b \in B/\{5-10°C\}} \lambda_{b,\text{Heat-Averse-Indicator}} \times \text{Tbin}_{r,t} \times \text{Heat-Averse-Indicator}_{it}^{r,s} + \boldsymbol{\delta}\mathbf{X}_{i,t} \\ & + \delta_i + \alpha_{s,r,t} + \varepsilon_{s,r,i,t}, \qquad \text{Heat-Averse-Indicator} \in \{\text{Small, No AC}\}\end{aligned} \tag{28}$$

where r denotes the region, s denotes a sector, i denotes the firm and t denotes the year. The indicator variable Heat-Averse-Indicator$_{it}^{s,r}$ is set to 1 if a firm is small or not AC-equipped. η_i is firm fixed effects and removes time-invariant, unobserved firm-level heterogeneity that could otherwise bias estimates of MRPK. $\alpha_{s,r,t}$ is sector-region-year fixed effects that removes the influence of unobserved characteristics specific to each region-sector pair in each year. Standard errors are clustered at region-level to account for serial and spatial correlation. The coefficients of interest: λ_b and $\lambda_{b,\text{Heat-Averse-Indicator}}$ are identified by comparing two firms within the same country-sector pair and exposed to the same temperature shocks, yet with different heat sensitivities. $\lambda_b > 0$ indicates an increase in MRPK for heat-tolerant firms when exposed to temperature shocks of bin b. $\lambda_{b,\text{Heat-Averse-Indicator}} < 0$ suggests a decrease in MRPK for heat-averse firms compared to heat-tolerant firms under the same temperature conditions. $\lambda_b + \lambda_{b,\text{Heat-Averse-Indicator}}$ represent the total effect of temperature shocks on heat-averse firms.

normality assumption.

Heterogeneous Effect of Temperature Shocks from Firm Size. Following the approach of Bau and Matray (2023), we characterize a firm's size using the value of its lagged capital stock. In each region-sector-year, firms are divided into two categories according to the following criterion: small firms, identified as those whose lagged capital stock falls below the median, and large firms, characterized as having a lagged capital stock above the median. We run equation 28 where Heat-Averse-Indicator$_{it}^{r,s}$:= Small$_{it}^{s,r}$, is set to 1 if a firm's lagged capital stock is less than the median in the region-sector-year.

Figure 5a plots the estimated impact of nine temperature bins on changes in MRPK. The impact of temperature conditions on the MRPK of small firms, plotted by the blue line, shows a decline across all temperature bins. In contrast, large firms, represented by the red line, only suffer statistically significant MRPK losses at extremely hot and cold temperatures. Comparatively, large firms enjoy a higher level of exhibit a relative increase in MRPK across various temperature ranges. The divergence of MRPK responses between large and small firms is most economically significant on extremely hot days with temperatures exceeding 30°C, confirming the most substantial impact on MRPK dispersion at extreme heat presented in Figure 2a. Detailed results are presented in Table F.5.

The results here validate our hypothesis that the difference in firm sizes is a source of $\hat{\beta}_i$ heterogeneity, and larger firms are more heat resistant. More interestingly, drawing back to our empirical findings on the heterogeneous impacts of extreme heat across different income levels, we find that wealthier economies suffer more from capital misallocation under extreme heat. This could be driven by the higher dispersion in firm sizes in richer economies, as documented by Poschke (2018) and observed in our data (Ivan said it'd be cool to actually plot this). We will revisit this in our exercises with aggregate data on the region-sector level.

Heterogeneous Effect of Temperature shocks from Adaptability. Another source of heterogeneity in $\hat{\beta}_i$ could be the differential adaptability to temperature extremes across firms. Naturally, we expect firms with greater adaptation measures to be more resilient to heat shocks and associated with a higher $\hat{\beta}_i$. We measure adaptability by the installments of the computerized air conditioning (AC) system, a variable collected in the Indian Annual Survey of Industries (ASI) every year since 2001. Our analysis for this part therefore focuses on the sample from Indian firms in ASI.

We run equation 28 where Heat-Averse-Indicator$_{it}^{r,s}$:= No AC$_{it}^{s,r}$, is set to 1 if a firm has no AC installment. The estimated effects are represented in Figure 5b. Firms with AC, indicated by the red line, experience negligible damage from extreme heat, whereas those without AC, represented by the blue line, show a noticeable decline in log MRPK when temperatures exceed the reference temperature. On the cooler spectrum, especially in temperatures below 5°C, both AC and non-AC firms see an increase in log MRPK. More precisely, as detailed in Table F.4, an additional day with temperatures falling below 5°C results in a 0.19% decrease in MRPK for firms without AC, compared to those with AC. For other cooler temperature ranges in India, specifically below 15-20°C, there is no significant difference in the MRPK between AC and non-AC firms. Conversely, at the higher temperature spectrum, particularly in ranges above 25-30°, including the 25-30°bin, there is a marked disparity in the MRPK between the AC and non-AC firms. An extremely hot day above 35°C, leads to a 0.4% decrease in the MRPK of firms lacking AC installations. We present the detailed results in Table F.4[28].

Figure 5: Effects of daily temperature shocks on log MRPK for firms of different sizes and adaptability

(a) Heterogeneous Effect from Firm Size (b) Heterogeneous Effect from Firm Adaptability

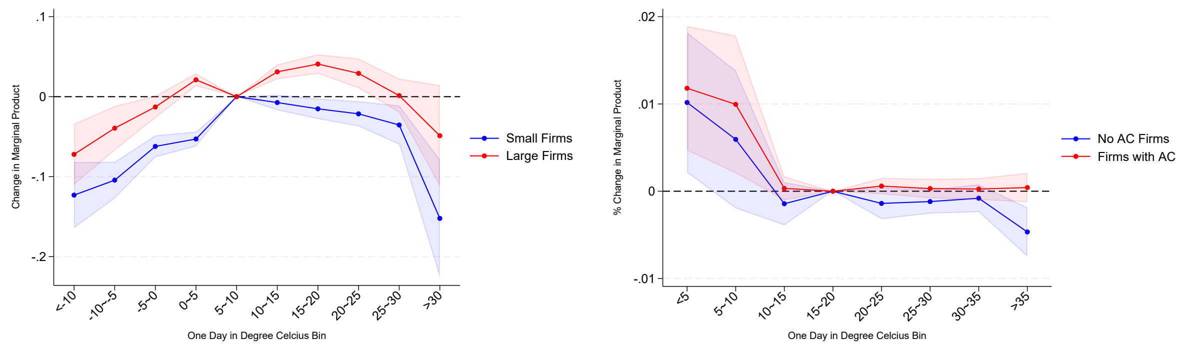

Notes: Graph plots the effects of daily mean temperature bins on firm-level log MRPK. Each point measures the estimated effect of an additional day in the temperature bin on log MRPK, relative to a day with temperatures between 5-10°C. FE are..., control variables are..., standard errors are clustered at ...

Might need to change what we plot here, which depends on what we want to show here.

28. Our baseline specification in Column 2 analyzes the within-firm variation on the effect of AC installation by including firm fixed effects δ_i and sector-year fixed effects $\theta_{s,t}$, and we include the AC indicator variable No $\text{AC}_{it}^{s,r}$ as controls. However, installing air conditioning is a common adaptation strategy for firms to cope with extreme heat, but it also makes them subject to costs of adaptive investment (e.g. Somanathan et al. 2021), which means the investment of AC itself could change the firm's MRPK as well. Following the approach of Asker, Collard-Wexler, and Loecker (2014), we address this in our alternative specification in Column (3) by conditioning on lagged TFPR and current capital stock to make sure that we are comparing two firms with the same lagged productivity making the same capital decision, but one firm has AC while the other does not. We include region-sector fixed effects and sector-year fixed effects in this specification, such that λ_b and $\lambda_{b,\text{No AC}}$ are identified based on the comparison of across-firm differences caused by AC installment within each region-sector.

7 Mechanisms of Climate-Driven Misallocation

In this section, we explore the micro-origins of climate-driven misallocation. We identify two mechanisms of misallocation suggested by the model in equation 26: (1) damage uncertainty and (2) climate volatility. We first validate the damage uncertainty channel by empirically estimating how temperature non-linearly changes the TFP volatility in the cross-section. We then provide evidence on the climate volatility channel by showing how forecast errors contribute to MRPK dispersion. Based on these estimates, we compute the relative contributions of uncertainty about damage sensitivity and volatility about climate warming to misallocation and find that damage uncertainty channel contributes most to misallocation.

$$\begin{aligned}\sigma^2_{mrpk,(r,s),t} &= \left(\frac{1}{1-\alpha_N}\right)^2 \text{Var}(\hat{a}_{nit} - \mathbb{E}_{t-1}[\hat{a}_{nit}]) \\ &= \left(\frac{1}{1-\alpha_N}\right)^2 \left[\underbrace{(T_{r,t} - T^*)^2 \sigma^2_{\xi,(r,s)}}_{\text{Damage Uncertainty Channel}} + \underbrace{\eta^{T\,2}_{r,t}\,\sigma^2_{\beta,(r,s)}}_{\text{Climate Volatility Channel}} + \sigma^2_{\varepsilon,(r,s)}\right]\end{aligned}$$

7.1 Mechanism 1: Damage Uncertainty

The relationship between TFP volatility and MRPK dispersion has been well studied. Therefore, we validate the connection between damage uncertainty and MRPK dispersion by first testing how damage uncertainty affects TFP volatility. Specifically, we measure the degree to which temperature shock might act like a "volatility shock" to firm-level productivity and then link it to misallocation via model-implied relationships later in 7.3.

Inspired by Equation 6(This equation reference seems a bit odd), we identify the nonlinear impact of temperature on TFP volatility from the following regression. We use the variance of the "first-differenced" TFP shocks, $\text{Var}_{nt}(\hat{a}_{it} - \hat{a}_{it-1})$[29]to approximate[30] the variability of unexpected TFPR shocks.[31]

$$\text{Var}_{(s,r),t}(\hat{a}_{it} - \hat{a}_{it-1}) = \alpha + \boldsymbol{\beta} \boldsymbol{f}(T_{r,t}) + \eta_{s,r} + \delta_{c(r),t} + \varepsilon_{s,r,t}, \tag{29}$$

where $\boldsymbol{f}(T_{r,t})$ is a polynomial of annual average temperature mention why it's suddenly annual average temperature. $\eta_{s,r}$ and $\delta_{c(r),t}$ denotes region-sector and country-year fixed effects respectively.

The 3rd-order polynomial analysis indicates some asymmetry of the effect around the critical point T^*. The same 1°C increase brings more damage in hotter climates than cooler cli-

29. Measuring firm-specific productivity shocks is challenging and sensitive to mis-specifications for the TFPR process. This is particularly true in our model, where firm-level productivity responds heterogeneously to temperature shocks. To address this, we adopt the approach of Asker, Collard-Wexler, and Loecker (2014), calculating a proxy of TFP shocks as the difference in firm-level TFP over time, represented as $\hat{a}_{it} - \hat{a}_{it-1}$. In line with the methodology of David and Venkateswaran (2019), we use the model-implied TFP in our specification: $\hat{a}_{it} = \log(P_{it}Y_{it}) - \alpha \log K_{it}$.

30. This approximation would be exact if (all components of) productivity were to follow a random walk pattern.

31. TFP can alternatively be derived as the conventional Solow residuals including labor. However, as noted in David and Venkateswaran (2019), footnote 22, TFP calculated from the Solow residual approach can no longer be directly tied to capital profitability in the presence of labor distortions, while the model-based measure of TFP remains a valid proxy for capital profitability.

mates. The U-shaped pattern from the cubic specification is plotted in Figure 6. In Appendix E.1 we discuss results from linear and quadratic specifications.

(A weird place to say this:) This temperature-volatility relationship, as depicted in Figure 4, also clarifies why hot temperature shock in cooler climates leads to a decrease in MRPK dispersion while producing an opposite effect in hotter climates.

Additionally, we apply the Delta Method to the estimated coefficients in the nonlinear specifications to determine the critical point T^* using formulas for quadratic and cubic functions. We find the bliss-point temperature at $\hat{T}^* = 13.82$ and $\hat{T}^* = 13.19$ for the quadratic and cubic specifications, respectively. Around 13°C, these figures align closely with those found in studies by Burke, Hsiang, and Miguel (2015) and Nath, Ramey, and Klenow (2023), who focused on country-level GDP. Our findings corroborate these findings by suggesting an additional mechanism: temperature shocks contribute to aggregate MRPK dispersion and TFP (output) loss as a second-moment shock[32].

Figure 6: TFP Volatility and Annual Average Temperature

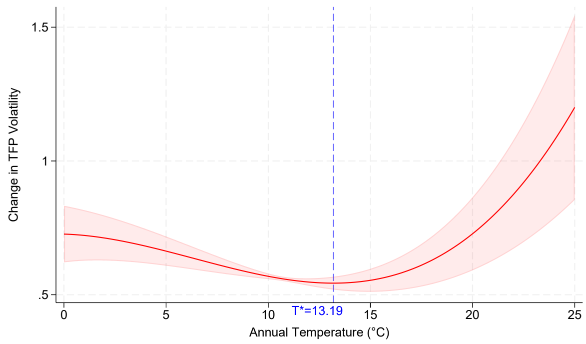

Notes: Graph plots the effects of temperature shocks on TFP volatility, based on a 3-rd order polynomial estimation derived from Equation 29. The asymmetrical pattern around the critical point $T^* = 13.19$ suggests that a 1°C in temperature increase inflicts greater damage in hotter climates than cooler ones.

7.2 Mechanism 2: Temperature Forecast Error, Climate Volatility and Misallocation

The climate volatility channel ties misallocation with forecast errors of temperature. Even in our model where all the firms face the same temperature forecast as common information, their knowledge of their exposure heterogeneity $\hat{\beta}_i$ would lead to differential investment decisions. Thus, any common forecast error would lead to dispersion in capital return. This is summarized as the climate volatility channel in equation 26.

We opt to utilize data directly from long-range (seasonal) temperature forecasts from ECMWF (Copernicus Climate Change Service and Climate Data Store 2018), instead of relying on prox-

32. This estimated effect is quantitatively large in the context of global warming projections. To illustrate, let us consider a simple back-of-the-envelope calculation using parameters from our model. Take, for example, a permanent increase from 16 °C to 20 °C, which aligns with an RCP 8.5 climate scenario projected for Southern Spain (*World Bank Climate Change Knowledge Portal* 2023). According to our model's damage uncertainty mechanism, this 4 °C increase would increase TFP Volatility by 4.24 log points. This increment translates into a 12.31 log points increase in MRPK dispersion using equation (26). Subsequently, under standard elasticity assumptions, this dispersion translates into a 7.6% loss in TFP.

ies or basic statistical models to estimate forecast errors for the company's weather predictions. Extensive research has demonstrated that accurate daily and seasonal temperature and weather forecasts can have significant impacts on adaptation behaviors (Shrader 2023) and mortality (Shrader, Bakkensen, and Lemoine 2023), as economic agents base their decisions on these signals. Therefore, we also assume that firms actively incorporate month-ahead weather forecasts into their learning processes[33].

Based on equation (26), it is evident that a larger squared forecast error in a region-sector leads to more capital misallocation. To test the effect of temperature forecast error on misallocation, we directly estimate the empirical version of Equation 26 with the following regression:

$$\begin{aligned}\sigma^2_{mrpk,(s,r),t} = &\sum_{q\in\{\text{specific seasons or quarters}\}} \theta_q \cdot MSFE_{q,r,t} + \gamma_1 T_{rt} + \gamma_2 T^2_{rt} \\ &+ \eta_{s,r} + \delta_{c(r),t} + \varepsilon_{s,r,t},\end{aligned} \tag{30}$$

where $MSFE_{q,r,t}$ represents mean squared forecast errors averaged over the time frame q in region r, categorized based on various time aggregations such as seasons or quarters. Each coefficient θ_q corresponds to the impact of a one unit increase in MSFE in the time frame q on annual capital misallocation.

The estimation results for various periods, including warm season, cold season, and individual quarters (Q1-Q4), are presented in Table 1. Column (1) shows that the annual MSFE averaged across all months, has a positive but statistically insignificant effect on MRPK dispersion. However, this measure may be too general to capture the variations within a year, such as the impact of forecast errors during days of extreme heat compared to generally cooler periods (as noted by Shrader, Bakkensen, and Lemoine (2023)). Therefore we examine the MSFE by seasons or quarters, and the effects of forecast errors become more distinct and statistically significant, particularly during warmer seasons (April to September). For example, in the warm period where extreme heat is more prone to happen, a one-degree Celsius average forecast error shock in summer would lead to a 1.4 log point increase in MRPK dispersion, compared to a perfect information counterfactual. This highlights the importance of accurate summer temperature forecasts for efficient capital allocation. Column 3 delves into the MSFE for temperature by quarters. The coefficients related to forecast errors in Q1, Q2, and Q4 are relatively small and noisy. In contrast, forecast errors in Q3, typically the hottest period in Europe, greatly impact capital misallocation. Specifically, compared to a no forecast error benchmark, a one-degree average forecast error in Q3 results in a 0.97 log points rise in MRPK dispersion, equating to an approximate 0.13% annual TFP loss.

Our findings suggest that inaccurate temperature expectations for an upcoming summer heatwave could result in disparate errors in investment decisions among companies with varying degrees of sensitivity to heat. This, in turn, could lead to divergent capital returns when the actual temperatures are realized, measured as MRPK dispersion across firms. These results

33. Since firm-level panel data has a mismatch between forecast horizons (month-ahead) and reporting frequencies (annual), we aggregate the average monthly forecast errors (including monthly squared forecast error) over several months to create a measure of expectation error and mean square forecast error (MSFE) over a longer period. This measure can be taken quarterly (e.g., Jan, Feb, March as Q1), biannually (April to September as warm seasons and the rest as cold seasons), or annually.

Table 1: Effects of MSFEs on MRPK Dispersion

	(1)	(2)	(3)
Annual MSFE	0.0080		
	(0.0050)		
$\text{MSFE}_{\text{Warm Season}}$		0.0140***	
		(0.0039)	
$\text{MSFE}_{\text{Cold Season}}$		-0.0024	
		(0.0033)	
MSFE_{Q1}			-0.0003
			(0.0022)
MSFE_{Q2}			0.0030
			(0.0028)
MSFE_{Q3}			0.0097***
			(0.0028)
MSFE_{Q4}			-0.0025
			(0.0023)
$T_{r,t}$	-0.1548***	-0.1602***	-0.1606***
	(0.0246)	(0.0247)	(0.0247)
$T^2_{r,t}$	0.0071***	0.0072***	0.0073***
	(0.0010)	(0.0010)	(0.0010)
Region-Sector FE	Yes	Yes	Yes
Country-Year FE	Yes	Yes	Yes
Observations	115,206	115,206	115,206
R^2	0.867	0.867	0.867

Notes: Standard MSEs in parentheses. We cluster standard MSEs at the regional level. The dependent variables are the MRPK dispersion calculated through the variance of MRPK across firms. These results are obtained by estimating Equation 30 under various specifications. Column 1 shows results using annual average MSFEs as the independent variable. Column 2 presents results based on MSFEs segmented into summer and winter periods. In Column 3, the estimation is extended to include MSFEs across all four quarters. The dataset for this analysis currently comprises countries from Europe.

$^{*}\ p < 0.10$, $^{**}\ p < 0.05$, $^{***}\ p < 0.01$

highlight the value of accurate temperature forecasts: accurate predictions enable firms make informed investment decisions and avoid costly mistakes.

7.3 Misallocation: Two Channels

The estimation from the two mechanisms provide us parameters to construct the deviation from ideal temperature T^*, and the unexpected shock from forecasts $\eta^T_{r,t}$. We use these parameters to estimate the implied variance of the common and idiosyncratic component of the marginal effect of temperature, $\sigma^2_{\xi,(s,r)}$ and $\sigma^2_{\hat{\beta},(s,r)}$. These enable us to compute the relative contributions of damage uncertainty channel and climate uncertainty channel to capital misallocation across European countries.

Recall that equation 26 in our model implies the following decomposition of MRPK dispersion:

$$\sigma^2_{mrpk,(s,r),t} = \left(\frac{1}{1-\alpha_N}\right)^2 \left[\underbrace{(T_{r,t} - T^*)^2 \sigma^2_{\xi,(s,r)}}_{\text{Damage Uncertainty}} + \underbrace{\eta^{T\ 2}_{r,t} \sigma^2_{\beta,(s,r)}}_{\text{Climate Uncertainty}} + \sigma^2_{\varepsilon,(s,r)} \right]$$

We now directly run the regression version of this:

$$\sigma^2_{mrpk,(s,r),t} = \kappa_1 (T_{r,t} - \hat{T}^*)^2 + \kappa_2 \hat{\eta}^{T\ 2}_{r,t} + \iota_{s,r} + \iota_{c(r),s} + \varepsilon_{s,r,t}, \tag{31}$$

where $(T_{r,t} - \hat{T}^*)^2$ are computed as the deviation of annual temperature from our estimated optimal temperature from Equation 29 ($\hat{T}^* = 13.18$). $\hat{\eta}^{T\ 2}_{r,t}$ is computed as the square of various measures of perceived shock in temperatures, including first-differenced temperature (as if temperature is perceived to be a random walk), residuals from the AR process similar to those constructed by Nath, Ramey, and Klenow (2023), as well as the (maybe use summer or warmer season MSFE here to be consistent with prior mechanisms results)annual MSFE from temperature forecast data. We include region-sector fixed effect, $\iota_{s,r}$, as well as country-year fixed effect, $\iota_{c(r),s}$.[34]

To determine the average elasticities, we run pooled regressions and report the estimated coefficients of equation (31) in Table 2[35]. We estimate $\hat{\kappa}_1$ to be around 0.006, indicating an average degree of damage uncertainty to be $\mathbb{E}[\sigma^2_{\xi,(s,r)}] \approx 0.00087$. We find $\hat{\kappa}_2$ to be around 0.019 to 0.032, suggesting an average dispersion of climate sensitivity $\sigma^2_{\hat{\beta}}$ to be around 0.0026 to 0.0046.

34. Through this regression, we can observe how the effects of the two channels manifest in practice. Using the model structure, we can see that our first parameter of interest, $\kappa_1 \approx \mathbb{E}\left[\left(\frac{1}{1-\alpha_N}\right)^2 \sigma^2_{\xi,(s,r)}\right]$, reflects the average degree of damage uncertainty in productivity across all region-sector pairs (scaled by the curvature of capital profitability). Our second parameter of interest is κ_2, which measures $\kappa_2 \approx \mathbb{E}\left[\left(\frac{1}{1-\alpha_N}\right)^2 \sigma^2_{\hat{\beta},(s,r)}\right]$, the average degree of dispersion in climate sensitivity across all region-sectors. (The following sentences are not clear)To interpret the regression coefficient in our model, we use $\tilde{\alpha}_N = 0.619$, the non-capital components of gross output scaled by $\sigma_n = 4$ which is obtained from the share of non-capital input in gross output of $1 - 0.35 \times 0.5 = 0.825$, adjusted by elasticity $\sigma_n = 4$, implying that $\left(\frac{1}{1-\alpha_N}\right)^2 = 6.89$.

35. We report the mean of temperature variables in the sample, including average squared deviation from "bliss point" $\overline{(T_{r,t} - T^*)^2}$, average squared AR-estimated residuals $\overline{\eta^{T\,2}_{t\ \text{AR}}}$, average first-differenced $\overline{(\Delta T_{r,t})^2}$ and average MSFE $\overline{MSFE_{r,t}}$ in the last row of Table 2.

Table 2: Estimated Effects of the Two Channels

	(1)	(2)	(3)
$(T_{r,t} - T^*)^2$	0.0060***	0.0058***	0.0061***
	(0.0012)	(0.0012)	(0.0012)
${\eta_t^T}^2_{\text{AR}}$	0.0313*		
	(0.0170)		
$(\Delta T_{r,t})^2$		0.0186***	
		(0.0071)	
$MSFE_{r,t}$			0.0072
			(0.0049)
Region-Sector FE	Yes	Yes	Yes
Country-Year FE	Yes	Yes	Yes
Observations	108,592	107,896	115,206
R^2	0.869	0.874	0.867
Average Temperature Variables across Europe in the sample:			
$\overline{(T_{r,t} - T^*)^2}$	$\overline{{\eta_t^T}^2_{\text{AR}}}$	$\overline{(\Delta T_{r,t})^2}$	$\overline{MSFE_{r,t}}$
15.854	0.145	0.569	2.317

Notes: Standard errors in parentheses. We cluster standard errors at the regional level. The dependent variables are MRPK dispersion. These results are obtained by estimating Equation 31.
* $p < 0.10$, ** $p < 0.05$, *** $p < 0.01$

With these estimates, we examine which of the two channels could be more prominent across the observed realizations in an average region sector in European countries. We compute the average contribution of the two channels to MRPK dispersion and implied TFP loss using the results of our baseline specification:

$$
\begin{aligned}
\overline{\Delta\sigma^2_{mrpk,(s,r),t}} &= \underbrace{\underbrace{\left(\frac{1}{1-\alpha_N}\right)^2 \hat{\sigma}^2_{\hat{\xi},(s,r)} \overline{(T_{r,t} - T^*)^2}}_{0.006\times 15.85}}_{\substack{\text{Damage Uncertainty}\\ =0.095}} + \underbrace{\underbrace{\left(\frac{1}{1-\alpha_N}\right)^2 \hat{\sigma}^2_{\hat{\beta},(s,r)} \overline{{\eta^T_{r,t}}^2}}_{0.031\times 0.145}}_{\substack{\text{Climate Uncertainty}\\ =0.0045}}, \\
\overline{\Delta \log TFP_{(s,r),t}} &= -\frac{(\sigma_n\tilde{\alpha}_K + \tilde{\alpha}_N)\,\tilde{\alpha}_K}{2}\overline{\Delta\sigma^2_{mrpk,(s,r),t}} \\
&= -\underbrace{\frac{(\sigma_n\tilde{\alpha}_K + \tilde{\alpha}_N)\,\tilde{\alpha}_K}{2}\frac{\hat{\sigma}^2_{\hat{\xi},(s,r)}}{(1-\alpha_N)^2}\overline{(T_{r,t} - T^*)^2}}_{\substack{\text{Damage Uncertainty}\\ =1.27\%}} \\
&\quad -\underbrace{\frac{(\sigma_n\tilde{\alpha}_K + \tilde{\alpha}_N)\,\tilde{\alpha}_K}{2}\frac{\hat{\sigma}^2_{\hat{\beta},(s,r)}}{(1-\alpha_N)^2}\overline{{\eta^T_{r,t}}^2}}_{\substack{\text{Climate Uncertainty}\\ =0.06\%}} \\
&= 1.33\%
\end{aligned} \tag{32}
$$

Through these back-of-envelope calculations, we find that, on average, the Damage Uncertainty channel contributes to 9.5 log points of MRPK dispersion, equivalent to a TFP loss of

1.27%. On the other hand, the Climate Uncertainty channel's contribution is bounded between 0.0045 and 0.06 log points, implying a TFP loss of 0.06%. Although rough, These estimates suggest that climate change's level effect would play a more significant role by creating greater uncertainty in productivity losses from temperature among firms.

References

Abel, Andrew B. 1983. "Optimal Investment Under Uncertainty." *The American Economic Review* 73 (1): 228–233. Accessed November 27, 2023.

Ackerberg, Daniel A., Kevin Caves, and Garth Frazer. 2015. "IDENTIFICATION PROPERTIES OF RECENT PRODUCTION FUNCTION ESTIMATORS." *Econometrica* 83 (6): 2411–2451. Accessed November 27, 2023.

Alves, Felipe, Greg Kaplan, Benjamin Moll, and Giovanni L. Violante. 2020. "A Further Look at the Propagation of Monetary Policy Shocks in HANK." *Journal of Money, Credit and Banking* 52 (S2): 521–559.

Asker, John, Allan Collard-Wexler, and Jan De Loecker. 2014. "Dynamic Inputs and Resource (Mis)Allocation." *Journal of Political Economy* 122 (5): 1013–1063.

Bakkensen, Laura A, and Lint Barrage. 2021. "Going Underwater? Flood Risk Belief Heterogeneity and Coastal Home Price Dynamics." *The Review of Financial Studies* 35 (8): 3666–3709.

Baqaee, David Rezza, and Emmanuel Farhi. 2019. "The Macroeconomic Impact of Microeconomic Shocks: Beyond Hulten's Theorem." *Econometrica* 87 (4): 1155–1203.

Barrage, Lint, and William D Nordhaus. 2023. *Policies, Projections, and the Social Cost of Carbon: Results from the DICE-2023 Model.* Working Paper, Working Paper Series 31112. National Bureau of Economic Research.

Basu, Susanto, and John G. Fernald. 2002. "Aggregate productivity and aggregate technology." *European Economic Review* 46 (6): 963–991.

Bau, Natalie, and Adrien Matray. 2023. "Misallocation and Capital Market Integration: Evidence From India." *Econometrica* 91 (1): 67–106.

Bigio, Saki, and Jennifer La'O. 2020. "Distortions in Production Networks*." *The Quarterly Journal of Economics* 135 (4): 2187–2253.

Bils, Mark, Peter J. Klenow, and Cian Ruane. 2021. "Misallocation or Mismeasurement?" *Journal of Monetary Economics* 124:S39–S56.

Blanchard, Olivier, and Jordi Galí. 2010. "Labor Markets and Monetary Policy: A New Keynesian Model with Unemployment." *American Economic Journal: Macroeconomics* 2, no. 2 (April): 1–30.

Burke, Marshall, Solomon M. Hsiang, and Edward Miguel. 2015. "Global non-linear effect of temperature on economic production." *Nature* 527 (7577): 235–239.

Caggese, Andrea, Andrea Chiavari, Sampreet Goraya, and Carolina Villegas-Sanchez. 2023. "Climate Change, Firms, and the Aggregate Productivity." Working Paper.

Carleton, Tamma, Amir Jina, Michael Delgado, Michael Greenstone, Trevor Houser, Solomon Hsiang, Andrew Hultgren, et al. 2022. "Valuing the Global Mortality Consequences of

Climate Change Accounting for Adaptation Costs and Benefits." *The Quarterly Journal of Economics* 137 (4): 2037–2105.

Carlsson, Mikael, Alex Clymo, and Knut-Eric Joslin. 2022. *Dispersion over the business cycle: Passthrough, productivity, and demand.* Technical report. Sveriges Riksbank Working Paper Series.

Carrillo, Paul, Dave Donaldson, Dina Pomeranz, and Monica Singhal. 2023. *Misallocation in Firm Production: A Nonparametric Analysis Using Procurement Lotteries.* Working Paper, Working Paper Series 31311. National Bureau of Economic Research.

Cascarano, Michele, Filippo Natoli, and Andrea Petrella. 2022. *Entry, exit and market structure in a changing climate.* MPRA Paper.

Casey, Gregory, Stephie Fried, and Matthew Gibson. 2022. "Understanding Climate Damages: Consumption versus Investment." Federal Reserve Bank of San Francisco Working Paper 2022-21.

Chahrour, Ryan, Kristoffer Nimark, and Stefan Pitschner. 2021. "Sectoral Media Focus and Aggregate Fluctuations." *American Economic Review* 111 (12).

Christidis, Nikolaos, Dann Mitchell, and Peter A. Stott. 2023. "Rapidly increasing likelihood of exceeding 50°C in parts of the Mediterranean and the Middle East due to human influence." *npj Climate and Atmospheric Science* 6, no. 1 (May 26, 2023): 45.

Copernicus Climate Change Service and Climate Data Store. 2018. *Seasonal forecast daily and subdaily data on single levels.*

Cruz, José-Luis, and Esteban Rossi-Hansberg. 2023. *The Economic Geography of Global Warming.*

David, Joel M., Hugo A. Hopenhayn, and Venky Venkateswaran. 2016. "INFORMATION, MISALLOCATION, AND AGGREGATE PRODUCTIVITY." *The Quarterly Journal of Economics* 131 (2): 943–1006. Accessed November 27, 2023.

David, Joel M., and Venky Venkateswaran. 2019. "The Sources of Capital Misallocation." *American Economic Review* 109 (7): 2531–67.

David, Joel M., and David Zeke. 2021. *Risk-Taking, Capital Allocation and Optimal Monetary Policy.* Technical report. Federal Reserve Bank of Chicago. Accessed November 27, 2023.

De Loecker, Jan, and Frederic Warzynski. 2012. "Markups and Firm-Level Export Status." *American Economic Review* 102, no. 6 (May): 2437–71.

Dell, Melissa, Benjamin F Jones, and Benjamin A Olken. 2012. "Temperature Shocks and Economic Growth: Evidence from the Last Half Century." *American Economic Journal: Macroeconomics* 4 (3): 66–95.

Deryugina, Tatyana, and Solomon Hsiang. 2017. *The Marginal Product of Climate.* Working Paper, Working Paper Series 24072. National Bureau of Economic Research.

Deschênes, Olivier, and Michael Greenstone. 2011. "Climate Change, Mortality, and Adaptation: Evidence from Annual Fluctuations in Weather in the US." *American Economic Journal: Applied Economics* 3 (4): 152–185.

Dundas, Steven J., and Roger H. von Haefen. 2020. "The Effects of Weather on Recreational Fishing Demand and Adaptation: Implications for a Changing Climate." *Journal of the Association of Environmental and Resource Economists* 7 (2): 209–242.

Fajgelbaum, Pablo D., Edouard Schaal, and Mathieu Taschereau-Dumouchel. 2017. "UNCERTAINTY TRAPS." *The Quarterly Journal of Economics* 132 (4): pp. 1641–1692. Accessed November 27, 2023.

Flynn, Joel P., and Karthik Sastry. 2023. *Attention Cycles.*

Gopinath, Gita, Sebnem Kalemli-Ozcan, Loukas Karabarbounis, and Carolina Villegas-Sanchez. 2017. "Capital Allocation and Productivity in South Europe." *Quarterly Journal of Economics* 132 (4).

Gorodnichenko, Yuriy, Debora Revoltella, Jan Svejnar, and Christoph T Weiss. 2018. *Resource misallocation in European firms: The role of constraints, firm characteristics and managerial decisions.* Technical report. National Bureau of Economic Research.

Hartman, Richard. 1972. "The effects of price and cost uncertainty on investment." *Journal of Economic Theory* 5 (2): 258–266. Accessed November 27, 2023.

Hopenhayn, Hugo A. 1992. "Entry, Exit, and firm Dynamics in Long Run Equilibrium." *Econometrica* 60 (5): 1127–1150.

Hsiang, Solomon. 2016. "Climate Econometrics." *Annual Review of Resource Economics* 8 (1): 43–75.

Hsieh, Chang-Tai, and Peter J. Klenow. 2009. "Misallocation and Manufacturing TFP in China and India." *Quarterly Journal of Economics* 124 (4): 1403–1448.

Kalemli-Ozcan, Sebnem, Bent Sorensen, Carolina Villegas-Sanchez, Vadym Volosovych, and Sevcan Yesiltas. 2015. *How to Construct Nationally Representative Firm Level Data from the Orbis Global Database: New Facts and Aggregate Implications.* Working Paper, Working Paper Series 21558. National Bureau of Economic Research.

Krusell, Per, and Anthony A. Smith Jr. 1998. "Income and Wealth Heterogeneity in the Macroeconomy." *Journal of Political Economy* 106 (5): 867–896.

Lemoine, Derek. 2018. *Estimating the Consequences of Climate Change from Variation in Weather.* Working Paper, Working Paper Series 25008. National Bureau of Economic Research.

Levinsohn, James, and Amil Petrin. 2003. "Estimating Production Functions Using Inputs to Control for Unobservables." *The Review of Economic Studies* 70 (2): 317–341.

Mérel, Pierre, and Matthew Gammans. 2021. "Climate Econometrics: Can the Panel Approach Account for Long-Run Adaptation?" *American Journal of Agricultural Economics* 103 (4): 1207–1238.

Moll, Benjamin. 2014. "Productivity Losses from Financial Frictions: Can Self-Financing Undo Capital Misallocation?" *American Economic Review* 104 (10).

Nath, Ishan. 2023. "Climate Change, The Food Problem, and the Challenge of Adaptation through Sectoral Reallocation."

Nath, Ishan, Valerie Ramey, and Peter Klenow. 2023. "How Much Will Global Warming Cool Global Growth?"

Oi, Walter Y. 1961. "The Desirability of Price Instability Under Perfect Competition." *Econometrica* 29 (1): 58–64. Accessed November 27, 2023.

Oudin Åström, Daniel, Bertil Forsberg, Kristie L. Ebi, and Joacim Rocklöv. 2013. "Attributing mortality from extreme temperatures to climate change in Stockholm, Sweden." *Nature Climate Change* 3, no. 12 (December 1, 2013): 1050–1054.

Ponticelli, Jacopo, Qiping Xu, and Stefan Zeume. 2023. *Temperature and Local Industry Concentration.* Technical report w31533. National Bureau of Economic Research.

Poschke, Markus. 2018. "The Firm Size Distribution across Countries and Skill-Biased Change in Entrepreneurial Technology." *American Economic Journal: Macroeconomics* 10 (3): 1–41.

Raimi, Daniel, Amelia Keyes, and Cora Kingdon. 2020. *Florida Climate Outlook: Assessing Physical and Economic Impacts through 2040.* Resources for the Future.

Restuccia, Diego, and Richard Rogerson. 2008. "Policy distortions and aggregate productivity with heterogeneous establishments." *Review of Economic dynamics* 11 (4): 707–720.

Rohde, Robert, Richard Muller, Robert Jacobsen, Saul Perlmutter, and Steven Mosher. 2013. "Berkeley Earth Temperature Averaging Process." *Geoinformatics Geostatistics: An Overview* 01 (02).

Rudik, I., G. Lyn, W. Tan, and A. Ortiz-Bobea. 2021. *The Economic Effects of Climate Change in Dynamic Spatial Equilibrium.*

Sabater, Joaquin Muñoz. 2019. *ERA5-Land monthly averaged data from 1950 to present.* Copernicus Climate Change Service (C3S) Climate Data Store (CDS).

Shrader, Jeffrey. 2023. "Improving climate damage estimates by accounting for adaptation." *Available at SSRN 3212073.*

Shrader, Jeffrey, Laura Bakkensen, and Derek Lemoine. 2023. "Fatal Errors: The Mortality Value of Accurate Weather Forecasts." National Bureau of Economic Research Working Paper.

Somanathan, E., Rohini Somanathan, Anant Sudarshan, and Meenu Tewari. 2021. "The Impact of Temperature on Productivity and Labor Supply: Evidence from Indian Manufacturing" [in en]. *Journal of Political Economy* 129 (6): 1797–1827. Accessed November 27, 2023.

Sraer, David, and David Thesmar. 2023. "How to Use Natural Experiments to Estimate Misallocation." *American Economic Review* 113 (4): 906–38.

World Bank Climate Change Knowledge Portal. 2023. https://climateknowledgeportal.worldbank.org/.

Zhang, Peng, Olivier Deschenes, Kyle C Meng, and Junjie Zhang. 2018. "Temperature effects on productivity and factor reallocation: Evidence from a half million Chinese manufacturing plants." *Journal of Environmental Economics and Management* 88:1–17.

Zivin, Joshua Graff, and Matthew Neidell. 2014. "Temperature and the Allocation of Time: Implications for Climate Change." *Journal of Labor Economics* 32 (1): 1–26.

A Accounting Framework

B Data

C Additional Empirical Results

C.1 Heterogeneous Effect Across Sectors

We further investigate how temperature might also pose differential effects on different sectors by estimating the specification in equation 13 for each sector's MRPK dispersion.

Figure C.1 presents the estimation for the six most common sectors in our sample. Consistent with the findings in Rudik et al. (2021) and Cruz and Rossi-Hansberg (2023), our study also identifies the agricultural sector as particularly susceptible to heat. We find that an additional day with temperatures exceeding 30°C impacts the dispersion of MRPK in agriculture by 2 log points, translating to 0.3% annual TFP loss. This heightened sensitivity might be primarily due to the heterogeneity of crops' sensitivity to weather and climate conditions. Extreme heat can adversely impact different crop yields and sales differentially, thus influencing firm productivity and MRPK dispersion within the sector.

The manufacturing sector is particularly susceptible to temperature, where extreme cold and hot conditions lead to increased MRPK dispersion (Zhang et al. 2018). This sensitivity in manufacturing might be attributed to the impact of extreme temperatures on production processes and worker productivity. Regarding the retail and service sectors, the U-shaped pattern in response to temperature variations is still observed and quantitatively important, although the results are less statistically significant. Interestingly, when using spatial variations in trade patterns to identify the productivity damage functions, Rudik et al. (2021) also find that the effect of heat on productivity loss is most prominent in agriculture sectors, followed by manufacturing sectors, and found a null effect in services, which is consistent with our findings on misallocation across sectors.

C.2 Dynamic Effects via Local Projection

Our theory suggests that historical weather realizations could influence the present misallocation. In other words, a one-time extreme weather shock could persistently impact misallocation.

In order to estimate the cumulative dynamic effects of temperature variations on capital misallocation, we estimate the local projection version of Equation 13 following Jorda (2005):

$$\begin{aligned} \mathrm{var}_{mrpk_{(s,r),t+h}} - \mathrm{var}_{mrpk_{(s,r),t-1}} = & \sum_{b \in B/(5\sim 10^{\circ}C)} \lambda^b_{\sigma^2_{mrpk},h} \times \mathrm{Tbin}^b_{r,t} + \boldsymbol{\delta}_{\sigma^2_{mrpk}} \mathbf{X}_{s,r,t} \\ & + \alpha_{c(r),t+h} + \eta_{s,r} + \varepsilon_{r,s,t+h} \end{aligned} \tag{33}$$

The coefficient $\lambda^b_{\sigma^2_{mrpk},h}$ measures the cumulative change of the dispersion of MRPK over the next h-period to an additional day in the temperature bin b (relative to the reference category). All lagged controls are included in $\mathbf{X}_{s,r,t}$, including one-period lagged binned daily

Figure C.1: Climate-induced Misallocation Across Major Sectors

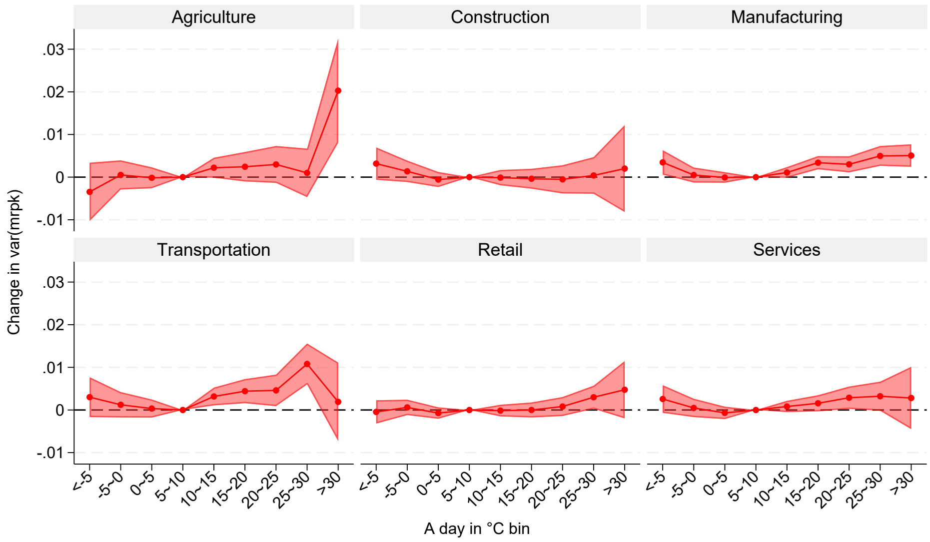

Notes: The graphs plot the estimated effect of exposure to daily mean temperatures on MRPK dispersion by estimating Equation 13 for six sectors, respectively. The graphs include 90% confidence intervals, and standard errors are clustered at the regional level.

temperature and one-period lagged MRPK dispersion. Notice that since past MRPK dispersion is independent of contemporaneous climate conditions, the coefficient $\lambda^{b}_{\sigma^2_{mrpk},h}$ measures the average total effect $\mathbb{E}\left[\frac{d\sigma^2_{mrpk_{(s,r)},t+h}}{d\mathbf{T}_{r,t}}\right]$.

We estimate Equation (33) with relative short horizons $h \in [-2, 3]$ due to the limited 20-year coverage of our data. Estimating with longer horizons could introduce lag truncation bias. Figure C.2 plots the estimates of $\lambda^{>30°C}_{\sigma^2_{mrpk},h}$ and $\lambda^{<-5°C}_{\sigma^2_{mrpk},h}$. In Figure C.2a, we observe that an additional day with temperatures exceeding 30°C leads to an immediate increase of 0.005 in MRPK dispersion, corresponding to a 0.07% loss of TFP. The effect gradually diminishes in subsequent periods. Figure C.2b shows that a further day with temperatures below -5°C results in a 0.002 unit increase in MRPK dispersion. The effects of cold days are weaker on impact but are more persistent, remaining at 0.002 after three periods.[36]

In order to formalize this within our accounting framework, which allows MRPK dispersion to be flexibly influenced by historical climate and economic conditions, we define the total marginal effect of climate conditions on a specific date t projected h period ahead MRPK dispersion as:

$$\frac{d\sigma^2_{mrpk_{(s,r)},t+h}}{d\mathbf{T}_{r,t}} = \underbrace{\sum_{l=0}^{h} \frac{\partial\sigma^2_{mrpk_{(s,r)},t+h}}{\partial\mathbf{X}_{s,r,t+l}} \frac{d\mathbf{X}_{s,r,t+l}}{d\mathbf{T}_{r,t}} + \sum_{l=0}^{h-1} \frac{\partial\sigma^2_{mrpk_{(s,r)},t+h}}{\partial\mathbf{T}_{r,t+l}} \frac{d\mathbf{T}_{r,t+l}}{d\mathbf{T}_{r,t}}}_{\text{Economic Persistence}} + \underbrace{\frac{\partial\sigma^2_{mrpk_{(s,r)},t+h}}{\partial\mathbf{T}_{r,t+h}} \frac{d\mathbf{T}_{r,t+h}}{d\mathbf{T}_{r,t}}}_{\text{Weather Persistence}} \tag{34}$$

We categorize all influencing factors into two channels: economic persistence and weather

36. Note that this estimate from "first differencing" is slightly smaller than the 0.09% estimate in our baseline specification reported in Table 1.

persistence. Economic persistence channels describe how the weather affects the dispersion of MRPK via intertemporal economic interactions. The first term in economic persistence captures how temperature conditions could affect future aggregate economic conditions, such as aggregate productivity and dispersion in productivity among firms, and, therefore, affects future misallocation through economic forces. The second term in economic persistence captures how the temperature conditions at date t (and the induced conditions up to $t + h - 1$) could directly affect the misallocation in the future (for example, through changes in investment in a long-term project). Finally, the weather persistence channel captures how weather conditions at date t could affect weather conditions at date $t + h$ (hence weather persistence), thereby contemporaneously affecting future MRPK dispersion. In general, it is not possible to estimate the economic persistence channel directly in a credible fashion. However, its effect can be netted out by subtracting the estimate of the weather persistence channel from the estimate of the cumulative dynamic effect $\frac{d\sigma^2_{mrpk_{(s,r)},t+h}}{d\mathbf{T}_{r,t}}$.

We can directly measure the weather persistence channel using the weather data. We find it to be small and statistically insignificant. We thereby conclude that the dynamic effect is caused by economic persistence instead. Potential factors that affect this could include adjustment costs, GE effects, noisy weather forecast revisions due to information frictions, and heterogeneous effects on capital depreciation.

Figure C.2: Estimated Dynamic Effect via Local Projection

(a) >30 °C Day (b) <-5 °C Day

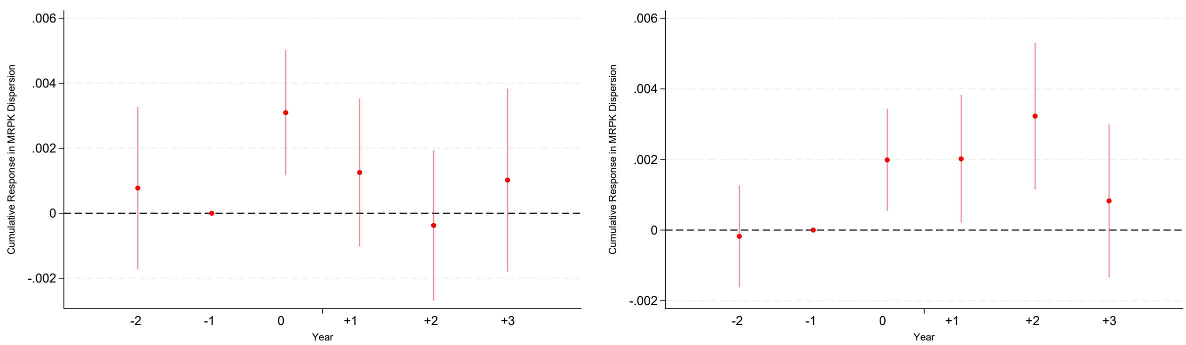

Notes: Graph plots the cumulative effect of temperature variations on capital misallocation with different future time h years later. The x-axis values are different $h \in [-2, 3]$. The $h = 0$ point shows the contemporaneous effect of temperature on MRPK dispersion. Panel C.2a plots the estimates of $\lambda^{>30^\circ C}_{\sigma^2_{mrpk},h}$. Panel C.2b plots the estimates of $\lambda^{<-5^\circ C}_{\sigma^2_{mrpk},h}$.

D Firm Dynamics Model

E Additional Mechanisms Results

E.1 Damage Uncertainty Additional Specifications

We discuss detailed results of the linear and polynomial estimation in Table E.5. Column (1) reports the linear estimation of the effects of temperature shocks, which is negative but not statistically significant. However, including second- and third-order terms reveals a remarkable nonlinear U-shaped pattern, aligning with our theoretical model. These nonlinear terms are not only statistically significant but also economically meaningful. Column (2) highlights that a 1 °C increase in the annual average temperature in a location with an average of 5°C leads to a decrease of 2.9 log points in TFP volatility. Conversely, the same 1 °C increase in a place with an average temperature of 20°C TFP volatility results in an increase of 2.5 log points in TFP volatility. Interpreting through our model, a positive temperature shock in a colder environment moves the economy closer to the optimal temperature T^*, reducing the harmful dispersion from idiosyncratic temperature damage $\hat{\xi}_{it}$. In contrast, the same positive shock in a hotter climate drives the economy further from T^*, increasing the uncertainty associated with climate damage.

Table E.5: Nonlinear Effects of Average Temperature on TFP volatility

	(1)	(2)	(3)
$T_{r,t}$	-0.0085	-0.0296***	-0.0024
	(0.0056)	(0.0099)	(0.0101)
$T^2_{r,t}$		0.0011**	-0.0028***
		(0.0005)	(0.0010)
$T^3_{r,t}$			0.0001***
			(0.0000)
Region-Sector FE	Yes	Yes	Yes
Country-Year FE	Yes	Yes	Yes
Implied $\hat{T}^*$		13.8138***	13.1885***
		(3.3034)	(1.1317)
Observations	107,427	107,427	107,427
R^2	0.746	0.746	0.746

Notes: Standard errors in parentheses. We cluster standard errors at the regional level. The dependent variables are TFP volatility. These results are obtained by estimating Equation 29. Column 1 presents the results of a linear estimation. Columns 2 and 3 present results with second and third-order polynomial estimations. The calculated critical temperature point $\hat{T}^*$ and its corresponding standard errors are calculated using the Delta Method.
* $p < 0.10$, ** $p < 0.05$, *** $p < 0.01$

F Tables

Table F.2: Effects of daily mean temperature bins on MRPK dispersion and TFP loss

	(1)	(2)	(3)	(4)	(5)	TFP loss
$< -5°C$	0.003***	0.003***	0.003***	0.003***	0.001	-0.037***
	(0.001)	(0.001)	(0.001)	(0.001)	(0.001)	(0.014)
-5∼0°C	0.002**	0.001**	0.002***	0.001***	0.001	-0.021**
	(0.001)	(0.001)	(0.001)	(0.001)	(0.001)	(0.008)
0∼5°C	0.000	0.000	0.001	0.000	-0.001	-0.005
	(0.000)	(0.000)	(0.000)	(0.000)	(0.001)	(0.006)
10∼15°C	0.001**	0.001**	0.001**	0.000	0.002**	-0.013**
	(0.000)	(0.000)	(0.000)	(0.000)	(0.001)	(0.005)
15∼20°C	0.002***	0.002***	0.002***	0.001**	0.003***	-0.022***
	(0.001)	(0.001)	(0.001)	(0.000)	(0.001)	(0.007)
20∼25°C	0.002**	0.002**	0.002**	0.001	0.002**	-0.023**
	(0.001)	(0.001)	(0.001)	(0.001)	(0.001)	(0.010)
25∼30°C	0.003***	0.003***	0.003***	0.002***	0.004***	-0.045***
	(0.001)	(0.001)	(0.001)	(0.001)	(0.001)	(0.014)
$> 30°C$	0.004***	0.004***	0.004***	0.003**	0.004***	-0.052***
	(0.001)	(0.001)	(0.001)	(0.001)	(0.002)	(0.018)
Controls	No	No	Yes	No	No	No
Region-Sector FE	Yes	Yes	Yes	Yes	Yes	Yes
Country-Year FE	Yes	No	Yes	No	No	Yes
Country-Sector-Year FE	No	Yes	No	Yes	Yes	No
Number of Firms Weighted	No	No	No	Yes	No	No
Average Sales Weighted	No	No	No	No	Yes	No
Observations	120,502	119,942	120,502	119,942	119,942	120,502
R^2	0.873	0.901	0.875	0.959	0.942	0.873

Notes: Standard errors in parentheses. We cluster standard errors at the region level (NUTS3 level for European countries, province level for China, and first-level administrative divisions for India). Dependent variables in Columns 1 to 5 are the variance of log MRPK. Columns 1 to 5 show results from estimating equation 13 with controls in Column 3 and two types of weight in Column 4 and 5. Column 6 shows results from the translation effect on MRPK to TFP loss (%) with formula $-\frac{\alpha_{Kn}+\alpha_{Kn}^2(\sigma_n-1)}{2}\hat{\lambda}^b_{\sigma^2_{mrpk}}$. Countries included are: China, India and 32 European countries.

$^{*}\ p < 0.10$, $^{**}\ p < 0.05$, $^{***}\ p < 0.01$

Table F.3: Effects of daily mean temperature bins on efficient TFP

	(1)	(2)	(3)	(4)
$< -5°C$	-0.00044***	-0.00021	-0.00052**	-0.00045***
	(0.00016)	(0.00015)	(0.00024)	(0.00016)
-5∼0°C	-0.00010	0.00001	-0.00054***	-0.00010
	(0.00010)	(0.00009)	(0.00015)	(0.00010)
0∼5°C	-0.00013	-0.00006	-0.00014	-0.00013
	(0.00008)	(0.00007)	(0.00011)	(0.00008)
10∼15°C	0.00012*	0.00007	0.00001	0.00012*
	(0.00007)	(0.00006)	(0.00011)	(0.00007)
15∼20°C	0.00004	-0.00005	-0.00005	0.00006
	(0.00009)	(0.00009)	(0.00014)	(0.00009)
20∼25°C	0.00011	-0.00010	0.00011	0.00013
	(0.00013)	(0.00012)	(0.00024)	(0.00013)
25∼30°C	-0.00004	-0.00016	-0.00044	-0.00004
	(0.00017)	(0.00016)	(0.00039)	(0.00017)
$> 30°C$	-0.00044	-0.00074**	-0.00090	-0.00038
	(0.00034)	(0.00035)	(0.00059)	(0.00033)
Number of Firms Control	No	Yes	No	No
Region-Sector FE	Yes	Yes	Yes	Yes
Country-Year FE	Yes	Yes	Yes	No
Country-Sector-Year FE	No	No	No	Yes
Average Sales Weighted	No	No	Yes	No
Observations	120,502	120,502	120,502	119,942
R^2	0.959	0.961	0.969	0.968

Notes: Standard errors in parentheses. We cluster standard errors at region level (NUTS3 level for European countries, province level for China, and first-level administrative divisions for India). Dependent variables are efficient TFP. Column 1 is the base line results and Column 2 introduces control variable of number of firms. Column 3 weight observations by average sales across firms in a region-sector. Countries included are China, India and 30 European countries.

* $p < 0.10$, ** $p < 0.05$, *** $p < 0.01$

Table F.4: AC Installment and Firm MRPK

	(1)	(2)	(3)
$< 5°C$	0.00682*	0.01221***	-0.00788*
	(0.00385)	(0.00446)	(0.00457)
5∼10°C	0.00347	0.00991**	0.00101
	(0.00320)	(0.00486)	(0.00163)
10∼15°C	0.00004	0.00050	0.00024
	(0.00061)	(0.00085)	(0.00065)
20∼25°C	0.00017	0.00064	0.00062
	(0.00052)	(0.00058)	(0.00055)
25∼30°C	0.00019	0.00029	0.00087*
	(0.00060)	(0.00068)	(0.00052)
30∼35°C	-0.00013	0.00025	0.00067
	(0.00069)	(0.00077)	(0.00054)
$> 35°C$	-0.00060	0.00030	-0.00026
	(0.00090)	(0.00104)	(0.00081)
$< 5°C \times$ No AC		-0.00156	-0.00194**
		(0.00172)	(0.00097)
5∼10°C $\times$ No AC		-0.00402	-0.00010
		(0.00424)	(0.00254)
10∼15°C $\times$ No AC		-0.00193	-0.00097
		(0.00139)	(0.00150)
20∼25°C $\times$ No AC		-0.00216**	-0.00117
		(0.00099)	(0.00079)
25∼30°C $\times$ No AC		-0.00152***	-0.00080*
		(0.00054)	(0.00044)
30∼35°C $\times$ No AC		-0.00106	-0.00110**
		(0.00068)	(0.00049)
$> 35°C \times$ No AC		-0.00483***	-0.00406***
		(0.00154)	(0.00137)
AC dummy	No	Yes	Yes
Control: $\ln TFPR_{t-1}$, $\ln K_t$	No	No	Yes
Region-Sector FE	No	No	Yes
Firm FE	Yes	Yes	No
Sector-Year FE	Yes	Yes	Yes
Observations	327,849	223,538	147,030
R^2	0.809	0.781	0.796

Notes: Standard errors in parentheses. We cluster standard errors at the firm level and region by year level. The dependent variables are the log MRPK. These results are obtained by estimating Equation **??**. Column 1 presents results that do not include interaction terms of the AC indicator variable. Columns 2 and 3 include the AC indicator variable. In addition, Column 3 incorporates control variables.

* $p < 0.10$, ** $p < 0.05$, *** $p < 0.01$

Table F.5: Firm Size and Firm MRPK

	(1)
< -10°C	-0.00072***
	(0.00023)
-10 ∼ -5°C	-0.00039**
	(0.00017)
-5 ∼ 0°C	-0.00013
	(0.00008)
0 ∼ 5°C	0.00021***
	(0.00005)
10 ∼ 15°C	0.00031***
	(0.00006)
15 ∼ 20°C	0.00041***
	(0.00007)
20 ∼ 25°C	0.00029***
	(0.00011)
25 ∼ 30°C	0.00001
	(0.00013)
$>$ 30°C	-0.00049
	(0.00038)
< -10°C × small	-0.00051***
	(0.00015)
-10 ∼ -5°C × small	-0.00065***
	(0.00016)
-5 ∼ 0°C × small	-0.00049***
	(0.00008)
0 ∼ 5°C × small	-0.00074***
	(0.00005)
10 ∼ 15°C × small	-0.00038***
	(0.00003)
15 ∼ 20°C × small	-0.00056***
	(0.00004)
20∼ 25°C × small	-0.00051***
	(0.00006)
25∼ 30°C × small	-0.00037***
	(0.00007)
$>$ 30°C × small	-0.00103**
	(0.00050)
Controls	Yes
Firm FE	Yes
Country-Sector-Year FE	Yes
Observations	44201069
R^2	0.934

Notes: Standard errors in parentheses. We cluster standard errors at the region level(NUTS3 level for European countries, province level for China, and first-level administrative divisions for India). The dependent variables are the log MRPK. These results are obtained by estimating Equation **??**. Column 1 presents results that interact with firm size.

* $p < 0.10$, ** $p < 0.05$, *** $p < 0.01$